

AMERICAN UNIVERSITY OF BEIRUT

HUMAN PRIMARY CELL-BASED IN VITRO BLOOD-
BRAIN BARRIER TO STUDY TOXOPLASMA GONDII
BRAIN INVASION AND DRUG SCREENING

by
ZEINAB ALI SHOKOR

A thesis
Submitted in partial fulfillment of the requirements
for the degree of Master of Science in Biomedical Sciences
to the Department of Anatomy, Cell Biology and Physiological Sciences
of the Faculty of Medicine
at the American University of Beirut

Beirut, Lebanon
August 2025

ACKNOWLEDGEMENTS

First and foremost, thank you, God, for your endless blessings and love, for placing me on the right path and guiding me in my journey.

I want to sincerely thank my supervisor, Dr. Marwan El-Sabban, for his invaluable guidance, support, and encouragement throughout this research. Being part of his lab for the past two years has been a true honor, where he not only taught us how to think and act like scientists but also shared life lessons that have shaped our perspectives. Thank you, Dr. Sabban, for everything. I will always be grateful for this opportunity.

I am also deeply grateful to my co-advisor, Dr. Hiba El-Hajj, for her guidance and support throughout this project. I would also like to thank Dr. Maguy Hamie and Ms. Shaymaa Itani for their ongoing support and valuable contributions to this project.

To my beloved lab colleagues, I am forever grateful for the joy, motivation, and unforgettable memories we have created together. Special thanks to Sara, my project partner, and my best friend Jihan for their unwavering support that eased the challenges of this journey.

Finally, to my family, Mama, Baba, and Zahraa, and my brother mohammad. Thank you for your endless love and support. I hope I always make you proud of me.

ABSTRACT OF THE THESIS OF

Zeinab Ali Shokor

for

Master of Science in Biomedical Sciences
Major: Neuroscience

Title: Human Primary Cell-Based *In Vitro* Blood-Brain Barrier to Study *Toxoplasma Gondii* Brain Invasion and Drug Screening

Background: *Toxoplasmosis* is one of the most widespread parasitic infections that affects approximately one-third of the human population and nearly 80% of the Lebanese population. It is caused by *Toxoplasma gondii* (*T. gondii*), an obligate intracellular protozoan parasite capable of crossing the blood-brain barrier (BBB) and forming cysts within the brain, leading to chronic toxoplasmosis (CT). CT can be associated with various neuropsychiatric behavioral disorders, primary neuropathies, brain tumors, and its reactivation is a life-threatening condition in immunocompromised patients. Despite advances in pharmacology, effective treatments for CT remain a significant challenge, primarily due to the selective permeability nature of the BBB, which restricts the delivery of most drugs into the central nervous system. Therefore, to address this issue, a physiologically relevant *in vitro* BBB model is essential to study the barrier selectivity and functionality, and to elucidate the mechanisms of *T. gondii* brain invasion, ultimately supporting the development of effective therapeutic strategies.

Aim: Our study seeks to develop a biomimetic *in vitro* BBB model using primary human aortic endothelial cells (HAECs) and Normal human astrocytes (NHAs), which are the key components of the neurovascular unit that forms the BBB. To enhance structural and functional integrity, the model incorporates porcine brain-derived extracellular matrix (ECM). This model will enable us to investigate *T. gondii* brain invasion and will facilitate the screening for potential therapeutic drugs.

Methods: The endothelial barrier was established under three different conditions: uncoated, Matrigel-coated, and Matrigel combined with porcine-derived brain ECM. Functional and molecular assays were conducted to evaluate barrier integrity, including trans-endothelial electric resistance (TEER) and permeability assays using fluorescent tracers such as Sodium fluorescein and Evans' Blue. Additionally, gene and protein expression analysis of tight junction markers such as ZO-1, Cx43, and CLDN-5 was performed using quantitative qRT-PCR, western blot, and immunofluorescence (IF). The pathway of tachyzoite dissemination through the endothelial barrier was visualized by live-imaging assay and further confirmed by transmigration assay of infected versus control THP-1 cells.

Results: Culturing of endothelial cells on brain ECM enhanced the expression of brain-specific tight junction proteins, including ZO-1 and CLDN-5. This upregulation improved barrier integrity, as evidenced by the significant increase in TEER values, in the brain ECM-based model compared to both control and Matrigel conditions. Additionally, this model exhibited reduced permeability of some molecular tracers,

underscoring the critical role of brain ECM in enhancing the functional properties of the barrier. For *T. gondii* results, the imaging revealed that tachyzoites utilize both the transcellular and "Trojan horse" mechanisms for crossing the barrier, with a marked predominance of the latter.

Conclusion: Developing an *in vitro* blood-brain barrier BBB model represents a vital step toward understanding the neuropathology of infections caused by *T. gondii*. Such models provide valuable insight into the parasite mechanisms of brain invasion and offer a promising platform for therapeutic development, while minimizing the use of *in vivo* models.

Key words: Blood-Brain Barrier, Extracellular Matrix, *in vitro* model, TJ proteins, neurodegenerative diseases, *Toxoplasma gondii*, Trojan Horse.

TABLE OF CONTENTS

ACKNOWLEDGEMENTS	1
ABSTRACT	2
ILLUSTRATIONS	7
TABLES	8
ABBREVIATIONS	9
LITERATURE REVIEW	12
A. The Blood-Brain Barrier Structure and Constituents	12
1. Cellular Components	13
2. Basement Membrane	15
B. Major Transport Pathways of Different Molecules Across the BBB	16
C. Challenges of Drug Delivery to the Brain	17
D. Pathogen's Virulence and Its Relevance to BBB Disruption	18
1. T. gondii Life Cycle and Routes of Transmission	18
2. Toxoplasmosis and Associated Diseases	20
3. Translocation of T. gondii into the Brain	21
4. Immune System Response to T. gondii Invasion of the brain	23
5. Available Treatments for Chronic Toxoplasmosis	23
E. Current In Vitro Models	24
AIM AND OBJECTIVES	28

MATERIALS AND METHODS	29
A. CELL CULTURE	29
1. ECVs-304 Cell Line.....	29
2. Human Aortic Endothelial Cells (HAECs).....	29
3. Normal Human Astrocytes (NHAs)	30
4. THP-1 CELLS	30
5. Tachyzoites	31
6. Cell Viability and Proliferation Assay	31
B. Porcine Brain Extracellular Matrix	32
1. ECM Extraction	32
2. ECM Protein Quantification	33
3. SDS-Polyacrylamide Gel Electrophoresis SDS-PAGE for ECM Proteins	33
C. Proliferation Assay	34
D. BBB Modelling.....	34
1. Co-culture of HAEC and NHA.....	35
2. Matrigel and ECM Composite Thickness Assessment.....	36
E. Evaluation of Barrier Integrity and Functionality.....	36
1. TEER	36
2. Permeability Assay Evan’s Blue (EB) and Sodium Fluorescein (NaF) permeability assay.....	37
3. Monocytes Transmigration Assay	37
F. Molecular Analysis and Junctional Protein Expression	38
1. Gene Expression Assessment by Quantitative Real-Time Polymerase Chain Reaction	38
G. Immunofluorescence for Phenotypic Characterization and Adherent Junctional Protein Localization	40
H. Protein Extraction and Western Blot	41

I.	T. gondii Invasion Assay	42
1.	Effect of Tachyzoite Infection on the Transmigration of Monocytes Through an Endothelial Barrier	42
2.	Live Cell Imaging of Tachyzoites Co-Cultured with THP-1 Cells on an Endothelial Barrier.....	43
J.	Drug Screening	44
RESULTS		45
A.	Optimization of the Blood-Brain Barrier In Vitro Model Using ECV-304 Cell Line	45
B.	Importance of Using Human Primary Cells for the <i>In Vitro</i> BBB Model:.....	46
C.	Characterization of ECM Extracted from Porcine Brain Tissue and ECM Dose Response on HAECs.....	47
D.	Modeling the Endothelial Monolayer with HAEC	49
1.	Functional Assays	49
2.	Molecular Assays.....	51
E.	Normal Human Astrocytes Maintenance and Co-culture.....	52
F.	T. gondii Dissemination Through an Endothelial Barrier	54
G.	Testing the Effect of Imiquimod Drug on HAEC Monolayer	56
DISCUSSION.....		57
REFERENCES		60

ILLUSTRATIONS

Figure

1. Schematic Representation of a Cross-Section of the Blood-Brain Barrier.....	13
2. schematic diagram of the different types of transport across the blood-brain barrier. (Created in https://BioRender.com)	17
3. Schematic Representation of the Life Cycle of <i>T. gondii</i>	20
4. Schematic Representation of the Different Pathways for <i>T. Gondii</i> Translocation into the Brain. (Created in https://BioRender.com)	22
5. Optimization of in Vitro BBB Using ECV-304 Cell Line.....	45
6. Immunofluorescence Images of 63X Magnification	46
7. ECM Extraction Analysis and Dose Response	48
8. Functional Assays Analysis of HAECs	50
9. Molecular Assays Analysis of ZO-1, Cx43, and CLDN-5 in HAECs	51
10. Optimization of Matrigel Concentration for co-culture of HAECs and NHAs.....	53
11. Tachyzoites Type I (RHHX strain) Extravasating Through the HAECs Monolayer	55
12. Live/Dead Assay of HAEC Treated and Untreated with Imiquimod.....	56

TABLES

Table

1. Different Models of the Blood Brain Barrier (Ferro et al., 2020; Saliba et al., 2018; Sivandzade & Cucullo, 2018; Stone et al., 2019).....	26
2. Seeding Density of Different Cell Lines Per cm ²	31
3. RT-qPCR Primer Sequences and Annealing Temperatures for the Studied Human Genes	40
4. Antibodies Used for Immunofluorescence.	41

ABBREVIATIONS

BBB	Blood-Brain Barrier
CNS	Central Nervous System
BMECs	Brain Microvascular Endothelial Cells
HAECs	Human Aortic Endothelial Cells
NHAs	Normal Human Astrocytes
THP-1	Human Monocytic Leukemia Cell Line
NVU	Neurovascular Unit
TJ	Tight Junction
ECM	Extracellular Matrix
JAMs	Junctional Adhesion Molecules
ZO-1	Zonula Occludens-1
CLDN 5	Claudin 5
PBS	Phosphate Buffer Saline
PFA	Paraformaldehyde
TEER	Trans-Endothelial Electric Resistance
GFP	Green Fluorescent Protein
<i>T. gondii</i>	<i>Toxoplasma gondii</i>
AT	Acute toxoplasmosis
CT	Chronic Toxoplasmosis
HFF	Human Foreskin Fibroblast
NaF	Sodium Fluorescein
EB	Evans Blue
RPMI	Roswell Park Memorial Institute
VCBM	Vascular Cell Basal Medium

CHAPTER I

INTRODUCTION

The Blood-Brain Barrier (BBB) is a cellular barrier that separates the central nervous system (CNS) from the vascular system [1]. It functions as a selective barrier that protects the brain from pathogens and harmful substances traveling through the bloodstream [2], while allowing the exchange of ions, oxygen, and essential nutrients needed for normal brain function [3]. In this way, it acts as both an anatomical and physiological shield vital for maintaining neuronal homeostasis [4]. However, when the integrity of the BBB is compromised, the CNS becomes susceptible to a range of neurodegenerative diseases, infectious insults, or tumor metastasis in the brain [5]. Furthermore, the restrictive nature of the BBB presents a significant challenge to drug delivery, as it prevents many therapeutic drugs from crossing into the brain, thereby limiting treatments for various neurological conditions [6].

Toxoplasma gondii, a widespread intracellular protozoan parasite, is estimated to affect one-third of the global population [7]. Its transmission to the human body usually occurs through the consumption of raw, undercooked meat or indirect contact with a cat's feces [8]. Once inside the host body, it can cross the BBB and establish chronic toxoplasmosis (CT) by forming cysts within the brain [9]. The latter is associated with primary neuropathies, neuropsychiatric and behavioral disorders, as well as brain cancer [10].

Therefore, studying the mechanism by which *Toxoplasma gondii* invades the brain is crucial for the development of targeted therapeutic strategies [11]. Various in vitro BBB models have been developed to recapitulate the physiological and molecular

properties of the in vivo BBB to study CNS neuropathies and to improve drug delivery across the brain [12].

CHAPTER II

LITERATURE REVIEW

A. The Blood-Brain Barrier Structure and Constituents

In the mammalian body, three cellular and acellular barriers safeguard the central nervous system: the meninges, the Blood-Brain Barrier, and the cerebrospinal fluid [13]. Each barrier has a significant role in maintaining the CNS's stable environment [14]. The meninges provide the brain and the spinal cord with physical protection, while the CSF nourishes the brain with essential nutrients and eliminates toxic wastes [15]. Among these, the blood-brain barrier has the most pivotal role in preserving the CNS's internal environment [14].

The Blood-Brain Barrier is a cellular barrier that separates the central nervous system from the vascular system[4]It functions as a selective barrier that protects the brain from pathogens and harmful substances that can enter through the bloodstream [2] while allowing the exchange of ions, oxygen, and essential nutrients between the brain tissue and the blood without compromising this protective shield [3]. In this way, it acts as both an anatomical and physiological barrier vital for maintaining normal neural activity [5].

To maintain neuronal homeostasis, dynamic signaling between the blood-brain barrier components and other cell types in the brain parenchyma creates a complex known as a Neurovascular Unit (NVU) [16]. The BBB is considered the main part of the NVU, mainly made up of a tightly packed monolayer of non-fenestrated brain microvascular endothelium. These cells are located on a basement membrane and supported by pericytes and astrocytic end-feet (Figure 1).

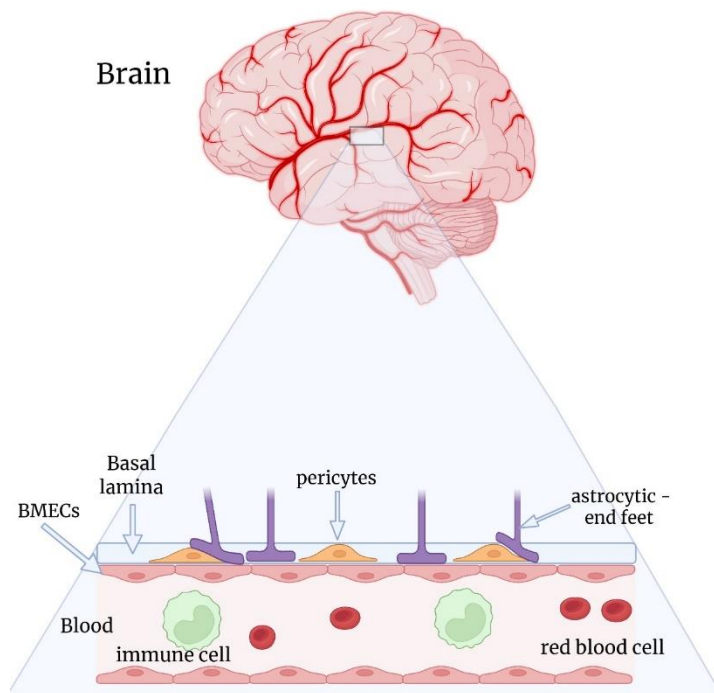


Figure 1: Schematic Representation of a Cross-Section of the Blood-Brain Barrier (Created in <https://BioRender.com>)

1. Cellular Components

a. Brain Microvascular Endothelial Cells

The BBB is primarily composed of brain microvascular endothelial cells (BMECs), which exhibit distinct structural and functional characteristics compared to peripheral endothelial cells [17]. These simple squamous endothelial cells, located at the interface between the bloodstream and the CNS [18, 19], are characterized by the presence of key junctional and adherent proteins, including claudins, VE-cadherin, and Occludin [20], which contribute to the maintenance of endothelial cohesion and restrict paracellular diffusion [16] [21]. In addition to limiting paracellular permeability, BMECs highly regulate transcellular transport and express a range of active efflux systems that prevent harmful substances from infiltrating the brain[22]. These cells exhibit reduced expression of leukocyte adhesion molecules, thereby limiting the transmigration of immune cells into the brain [23]. Furthermore, BMECs secrete

Glycocalyx, a mesh layer of polysaccharides that envelops the vascular lumen, serving as a functional barrier by restricting the diffusion of charged plasma proteins and functioning as a molecular filter. [23, 24].

b. Astrocytes

Astrocytes are the most abundant glial cells in the CNS [25]. They have a star-shaped structure with many fine processes called astrocytic end-feet, which surround brain microvessels [26] Recent research has highlighted the role of these end-feet as key regulators of brain metabolism [27]. They control water and ion exchange across the BBB through potassium channels and the water channel aquaporin 4 (AQP-4) [28]. Recent studies have shown a significant decrease in the density of these channels after disruption of the connection between the astrocytic end-feet and the basement membrane [27]. Additionally, astrocytes release various proteins such as basic fibroblast growth factor (BFGF), vascular endothelial growth factor A (VEGF-A), and angiotensin II, which influence the expression and location of tight junction (TJ) proteins in endothelial cells to regulate BBB permeability and maintain normal functions [29] Notably, in cases of encephalitis, reactive astrocytes contribute to glial scar formation around the barrier, limiting the infiltration of inflammatory immune cells into CNS tissue. This explains how the loss of astrocytes could lead to significant lymphocyte entry into the brain [30].

c. Pericytes

Pericytes, also known as vascular mural cells, are flattened, contractile, undifferentiated cells that surround vascular endothelial cells and are embedded within the same basement membrane ([31]. These mural cells, which mainly originate from

mesenchymal tissue, are spread throughout the vascular system in varying proportions, with the CNS showing the highest perivascular ratio. Pericytes play a crucial role in maintaining the integrity of the BBB and its selective permeability by regulating cerebral blood flow through the expression of alpha-smooth muscle actin [31] and by limiting immune cell infiltration into the brain parenchyma [32]. Besides their barrier-regulating function, pericytes are essential in angiogenesis, primarily due to their close and stable interaction with endothelial cells. For example, growth factors like PDGF-BB, released by vascular endothelial cells, encourage the migration and growth of pericytes into new blood vessels. Recent research shows that a reduction in pericyte numbers leads to increased permeability and loss of BBB integrity [31].

2. Basement Membrane

One of the NVU's non-cellular components is the basement membrane [5]. A unique three-dimensional protein matrix lies beneath the vascular endothelial cells, surrounding both pericytes and the astrocyte end-feet [27]. Ranging from 20 to 200 nm in thickness, it consists of several types of extracellular matrix (ECM) proteins, mainly collagen type IV, nidogen, laminin sulfate, and proteoglycans, which are synthesized and deposited by BBB components [33]. Notably, at the level of the postcapillary venule, the vascular basement membrane comprises two distinct layers: the endothelial basement membrane and the parenchymal basement membrane. Each has a unique ECM composition while sharing the crucial role of maintaining the integrity of the NVU's cellular components [5]. While most research highlights the importance of the NVU's cellular elements in restricting BBB permeability, some studies emphasize the basement membrane's key roles in mechanical protection, signaling pathway transduction, and

regulation of intracellular crosstalk among NVU components [34]. For example, the interaction between beta-1 integrin, expressed by BMECs, and collagen IV in the basement membrane promotes the expression of CLDN-5 TJ protein, supporting BBB integrity [33]. Consequently, disruption of this layer results in BBB impairment and loss of cellular interactions [35].

B. Major Transport Pathways of Different Molecules Across the BBB

Transport of molecules across the BBB occurs through two main routes: paracellular and transcellular [36]. In the paracellular route, molecules that are smaller than 70kDa pass through small gaps between the specialized TJs of neighboring endothelial cells because of the low permeability of the BBB [37]. The primary TJs at the BBB include the claudin family, especially CLDN-5, and Occludin, like zonula occludens-1 and junctional adhesion molecules (JAMs)[38]. Claudins have an important role in tightening the BBB and restricting the permeability of small molecules [37]. Additionally, Occludin helps reinforce barrier integrity by interacting with the cell's cytoskeleton through scaffolding proteins, serving as sensors and protectors against insults like hypoxia. On the other hand, transcellular routes involve several transport modes depending on the size and chemical nature of the solute [39]. The first mode is passive diffusion, where gases like oxygen, ions, and small lipophilic molecules pass through the lipid bilayer of endothelial cells [40]. Larger lipophilic substances like cholesterol that cannot passively diffuse through the BBB are actively transported by energy-dependent ATP-binding cassette (ABC) transporters, like ABCB1 or P-glycoprotein [41]. Furthermore, solutes like glucose, neurotransmitters, and various amino acids rely on active transport via carrier-mediated proteins located on the

endothelial cell membranes [39]. Another mode of transport is transcytosis, which involves the targeted transport of macromolecules by binding to membrane receptors and forming caveolae for engulfment into the cell [42] (Figure 2).

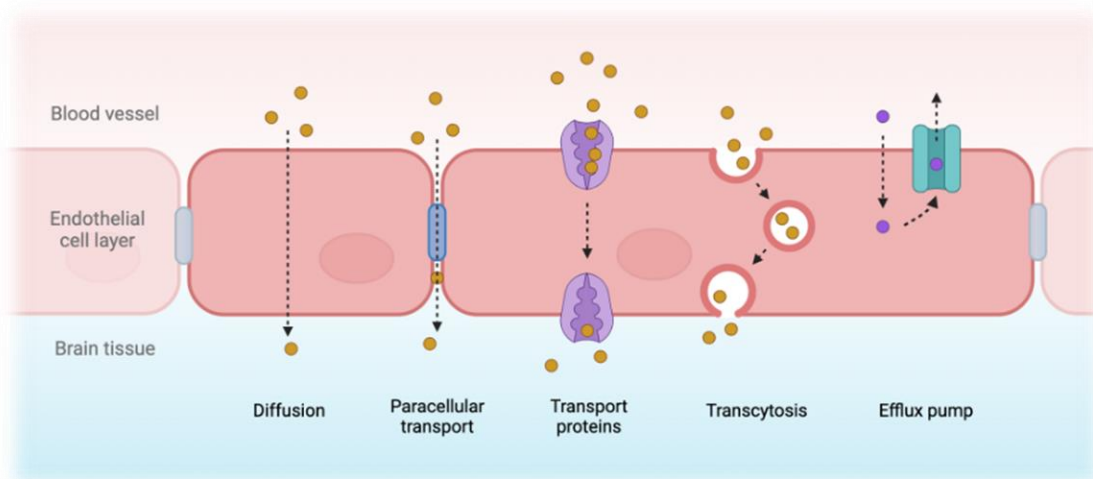


Figure 2: schematic diagram of the different types of transport across the blood-brain barrier. (Created in <https://BioRender.com>)

Small molecules (<70 KDa) pass paracellularly between adjacent endothelial cells. While other molecules are transported through the transcellular route. Lipophilic molecules quickly diffuse through the cells. Larger lipophilic molecules and nutrients depend on active transport, in addition to transcytosis, which is divided into specific receptor-mediated transcytosis and nonspecific absorptive-mediated transcytosis.

C. Challenges of Drug Delivery to the Brain

CNS diseases, from gliomas to neurological disorders, are considered among the top global health concerns due to the CNS's complex protective structure, especially with the presence of the BBB [43]. This cellular barrier hinders the entry of various molecules and chemicals into the brain, including medications and therapies that target brain diseases. Recent studies have shown that up to 98% of drugs are unable to pass through the BBB. The migration of drugs across the BBB depends on their physicochemical properties, such as molecular weight and charge. Small, lipophilic molecules with low

molecular weight can passively cross the lipid bilayer of BMECs; in contrast, large drug molecules face greater difficulty in penetrating the BBB [44]. Additionally, some drug molecules are subjected to active efflux by being transported back to the bloodstream by the action of ATP-binding cassette proteins like P-glycoprotein, which further restricts their access to the brain [45]. Several technologies have been developed to facilitate the delivery of drugs into the brain like nanoparticles, liposomes, transport through immune cells, and many other methods that have shown success in transporting the drug through the BBB [46], however, these strategies disrupted the blood-brain barrier, damaged the brain tissue and possessed risks to irreversible damage to the barrier's permeability [47]. Therefore, an effective blood-brain barrier model is crucial for studying the BBB's selective permeability and functional properties, thereby improving our understanding of neurological disorders and aiding the development of targeted drug strategies.

D. Pathogen's Virulence and Its Relevance to BBB Disruption

1. T. gondii Life Cycle and Routes of Transmission

Toxoplasma gondii, an obligate intracellular protozoan parasite capable of infecting a wide range of warm-blooded hosts, including one-third of the world's human population [48]. The prevalence of *T. gondii* infection varies by region and can reach an alarming 80% in certain areas [49]. As a major zoonotic pathogen [50], the parasite exhibits three distinct phases: tachyzoites, bradyzoites, and sporozoites [51]. The latter, sporozoites, are an oocyte form of the parasite that can be transmitted to humans through consuming undercooked meat or contaminated water [52]. While tachyzoites, a fast-replicating form of *T. gondii* found in intermediate hosts like humans, are capable of invading various tissues throughout the body [53] the infection progresses as tachyzoites

differentiate into bradyzoites, the slow-growing yet most pathogenic stage. These bradyzoites form long-lasting dormant cysts within tissues, particularly in the brain, which serves as a significant organ of encystment and persistence [9] (Figure 3).

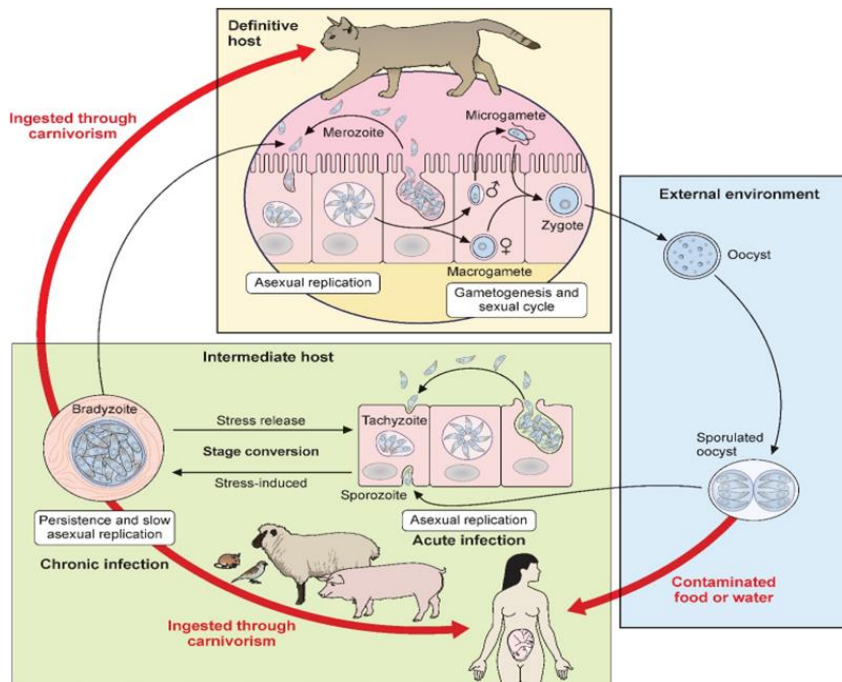


Figure 3: Schematic Representation of the Life Cycle of *T. gondii*

Infective stages of *T. gondii* and their modes of transmission and replication in their respective hosts [49]. The sexual phase occurs in the intestinal epithelium of cats, where the parasite produces oocysts. These oocysts are excreted into the environment, and they become infectious, leading to an asexual cycle if ingested by intermediate hosts. Tachyzoites cause an acute infection in intermediate hosts, then form latent bradyzoite cysts, which are responsible for the chronic disease.

2. *Toxoplasmosis and Associated Diseases*

Toxoplasmosis, an infection caused by the *T. gondii* parasite, affects both immunocompetent and immunosuppressed individuals [54]. In healthy hosts, toxoplasmosis manifests as acute and chronic forms. The acute phase of infection is typically asymptomatic in most cases, while the chronic phase is established when the parasite forms cysts within tissues, primarily the brain. [55] in immunocompromised patients, these cysts may reactivate, leading to potentially life-threatening conditions such as brain lesions known as toxoplasmosis encephalitis [56]

Moreover, several studies have shown that *T. gondii* is associated with multiple primary neuropathies and behavioral disorders [57]. Various research studies have

investigated the link between epilepsy and *T. gondii* infection, showing that cryptogenic epilepsy is associated with a significant increase in *T. gondii* IgG antibodies compared to controls and other epilepsies. Similarly, the seroprevalence of the parasite has been higher in Alzheimer's patients than in control groups [58]. Moreover, new studies have shown that infection with the parasite might lead to behavioral disorders like schizophrenia, depression, and suicidal attempts [58, 59].

3. Translocation of T. gondii into the Brain

For any pathogen to enter the CNS, it must cross the BBB. However, some pathogens like *T. gondii* have evolved mechanisms to breach this barrier and cause infections [55]. While the exact process of *T. gondii* brain invasion is not fully understood, studies have identified three main pathways for the dissemination of tachyzoites into host tissue [11]. The first pathway, the transcellular route, involves tachyzoites using gliding motion to invade endothelial cells lining the barrier, where they replicate and then exit through the basolateral side into the basement membrane. Alternatively, in the paracellular route, the parasite transmigrates between neighboring endothelial cells by interacting with tight junction (TJ) proteins, disrupting intercellular communication [55]. Additionally, a newly proposed mechanism called the “Trojan horse” route involves tachyzoites acting as hitchhikers within infected migratory leukocytes, mainly monocytes and dendritic cells [60] (Figure 4). This infection induces a hypermotility phenotype, facilitating dissemination and increasing adhesion to the endothelial barrier [61]. Moreover, *T. gondii* secretes proteins from micronemes, dense granules, and rhoptries that manipulate host cell signaling, cytoskeletal dynamics, and immune responses to ensure successful crossing of biological barriers [62]. For example,

the ROP17 kinase, released by *T. gondii*, contributes to its dissemination by modulating monocyte migration into tissues [63]. The virulence of *T. gondii* varies among strains (Type I, II, and III), mainly due to differences in expression of ROP kinases like ROP17 and ROP18, which influence the ability to breach the BBB [55]. Despite these findings, the process of *T. gondii* translocation into the CNS, the stage of infection, and whether it disrupts the BBB's restrictive permeability remain unknown. Therefore, non-invasive in vitro BBB models are necessary to develop platforms for studying *T. gondii* invasion and translocation, as well as to screen for potential brain-permeable drugs targeting this parasite.

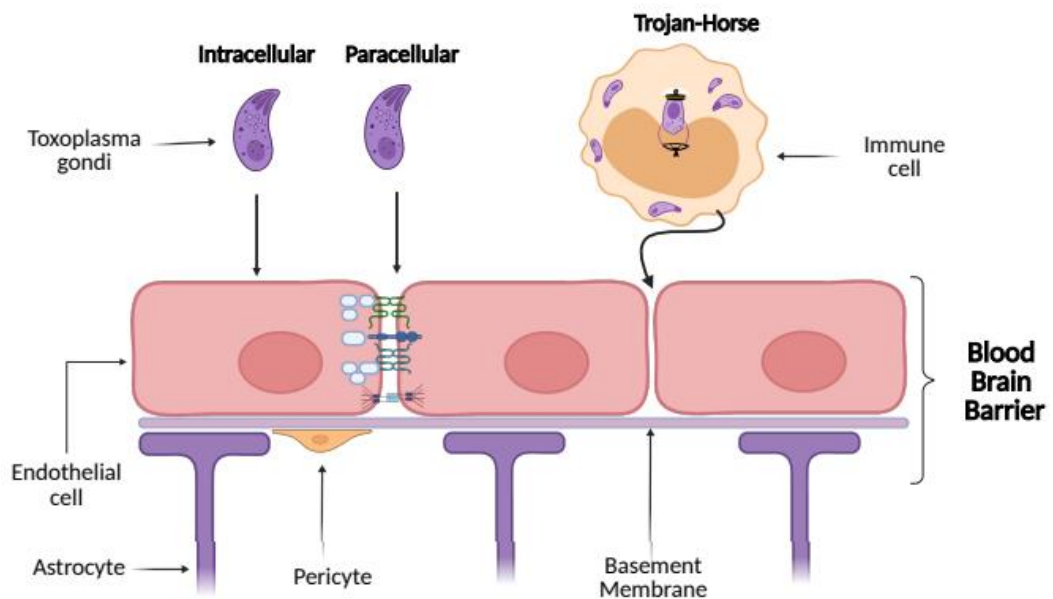


Figure 4: Schematic Representation of the Different Pathways for *T. Gondii* Translocation into the Brain. (Created in <https://BioRender.com>)

4. Immune System Response to T. gondii Invasion of the brain

Infection with *T. gondii* triggers a complex interaction between the parasite and the host immune system, especially in the CNS, where the immune response to *T. gondii* involves both innate and adaptive responses [64]. When infected with *T. gondii*, the host immune response begins with the recognition of the parasite by transmembrane Toll-like receptors (TLRs) expressed on the surface of monocytes, neutrophils, and dendritic cells (DCs), leading to the production of pro-inflammatory cytokines like IL-12. This cytokine stimulates natural killer (NK) cells and T cells to secrete IFN-gamma. The latter is essential for controlling the infection, as it activates macrophages, astrocytes, and microglial cells to inhibit parasite replication through mechanisms such as nitric oxide (NO) production and tryptophan starvation [65].

Followed by adaptive immunity, particularly CD4⁺ and CD8⁺ cells. CD4⁺ cells, along with astrocytes, contribute to resistance and activation of CD8⁺ cells, which in turn mediate protection against the parasite by releasing cytokine factors like IFN gamma to prevent tachyzoite proliferation, engaging in the CD40/CD40L interaction to promote immunity, and using perforin-mediated mechanisms to eradicate cysts through cytotoxic T cells [55].

5. Available Treatments for Chronic Toxoplasmosis

To date, treatments for toxoplasmosis are still limited to general anti-parasitic and anti-bacterial drugs, such as a combination of Sulfadiazine and Pyrimethamine, which are used as first-line treatments for toxoplasmosis due to their ability to disrupt the parasite's growth and activity by inhibiting folate biosynthesis in *T. gondii* [66]. However, this combination has been shown to target only the tachyzoite stage of the parasite and is

unable to effectively target bradyzoite cysts. Additionally, some therapeutic medicines have been developed to specifically target the parasite's organelles, such as the apicoplast or micronemes. Yet, later in in vivo studies, they exhibited several side effects, including skin rashes, hematological conditions, and organ toxicity. They also primarily target the acute stage of toxoplasmosis and are ineffective during the chronic stage [67]. On the other hand, researchers developed an immunomodulatory drug called imiquimod to combat toxoplasmosis by regulating the TLR-MyD88 signaling cascade. It boosts the immune response by triggering TLR recognition of profilin, a *Toxoplasma* pathogen-associated molecular pattern (PAMP), and activates T cells via MyD88 signaling [68]. More importantly, studies on imiquimod's efficacy against CT showed a dramatic reduction in brain cysts of infected mice, delayed reactivation, and reduced disease burden [69]. However, imiquimod is still not fully effective, as it can cause potential side effects in treating chronic toxoplasmosis, such as excessive immune activation leading to detrimental inflammatory responses, and its reliance on parasite PAMPs due to the presence of different strains [68]. Therefore, alternatives with improved bioavailability are being developed to address these challenges

E. Current In Vitro Models

Neuropathological diseases pose a major global challenge due to increasing mortality rates; their severity arises from the complexity of the CNS microenvironment and the BBB, which hinders therapeutic delivery [70]. Therefore, reliable in vitro models are necessary to study these diseases and evaluate potential treatments.

Animal-based in vivo models have been fundamental to advancing our understanding of brain tissue physiology and the phenotypic characteristics of various

CNS diseases [71]. While they remain indispensable tools in biomedical research, species-specific differences in genetics, molecular pathways, and protein expression can limit the translation of these findings to human biology [72]. As a result, these limitations, along with ethical concerns and the high costs associated with these models, have encouraged the use of in vitro models as a more efficient alternative [39]

As mentioned earlier, the urgent need for a reliable and effective platform to replicate the BBB has led to the development of various in vitro BBB models, including monoculture, 2D co-culture on trans-well, 3D organ-on-a-chip modeling, and microfluidic models [73]. Although these models vary in design and functionality, they share a common principle: culturing endothelial cells on a gel that mimics the basement membrane, placed on a semipermeable membrane between two liquid compartments to simulate the luminal and abluminal sides of the BBB [74]. Additionally, co-culturing different NVU cells, such as astrocytes and pericytes, improves the model's resemblance to the in vivo microenvironment [12] In vitro models differ not only in their design but also in the types of cells cultured, such as immortalized cells, primary human cells, or pluripotent stem cells. Furthermore, the choice of culture method—monoculture, co-culture, or 2D and 3D models—significantly impacts the properties and functionality of the model [75].

To date, the trans-well co-culture remains the most widely used in vitro model due to its simplicity, low resource requirement, and ability to measure BBB tightness and integrity [76]. It operates as a side-by-side vertical diffusion apparatus with a microporous semipermeable membrane that separates cells in apical compartments from basal ones, enabling the co-culture of brain microvascular endothelial cells from other NVU cells like astrocytes and pericytes [77]. Additionally, it can quantify genes associated with

barrier tightness and serve as a platform to study the invasion of different cells and molecules [78].

Table 1: Different Models of the Blood Brain Barrier (Ferro et al., 2020; Saliba et al., 2018; Sivandzade & Cucullo, 2018; Stone et al., 2019)

In vitro BBB models	Components	Advantages	Disadvantages
Petri dish	Static monoculture of one cell type (mainly Endothelial cells)	<ul style="list-style-type: none"> ○ very low-cost ○ quite simple fabrication, easy microscopic visualization of cells, and the ability to assess cell cytotoxicity 	<ul style="list-style-type: none"> ○ Unfeasible study of molecular transportation no shear stress
Trans-wells	2D coculture of monolayer EC on a semipermeable membrane and other cell types on either side	<ul style="list-style-type: none"> ○ low cost ○ simple fabrication, ability to study drug transportation and invasion assays ideal for linear kinetic studies 	<ul style="list-style-type: none"> ○ no shear stress ○ low TEER (permeability of polar molecules)
Spheroid	3D coculture of one and more cell types (EC, astrocytes...) using gel	<ul style="list-style-type: none"> ○ moderate cost ○ no scaffold ○ ability to study drug transportation and invasion assays 	<ul style="list-style-type: none"> ○ require technical skills not able to measure permeability
Dynamic	3D coculture of EC monolayer on the luminal side of a hollow fiber and other cell types on the other side of the membrane	<ul style="list-style-type: none"> ○ moderate cost ○ shear stress ○ ability to study drug transportation and invasion assays ○ high TEER ○ high restricted permeability 	<ul style="list-style-type: none"> ○ time consuming ○ require technical skills, need big cellular load, not able to visualize the intraluminal compartment
Organ-on-chip	3D coculture monolayer EC and other cell types in microfluidic channels fabricated using soft lithography techniques	<ul style="list-style-type: none"> ○ High cost ○ realistic dimensions and geometries ○ exposing the endothelium to physiological fluid flow, allow cells to be visualized microscopically 	<ul style="list-style-type: none"> ○ requires technical skills lack of standardized parameters, and quantification of critical experimental factors (luminal shear stress, TEER, permeability) ○ not ideal for linear kinetic studies

Microfluidics via 3D printing	3D coculture of monolayer EC and other cell types in a microfluidic channel, fabricated digitally	high cost ○ moderate fabrication ○ requires low cell load shear stress allow cells visualization microscopically	require technical skills not ideal for linear kinetic studies
--	---	---	--

CHAPTER III

AIM AND OBJECTIVES

This project aims to develop a physiologically relevant *in vitro* blood-brain barrier using human primary cell lines, like human aortic endothelial cells (HAEC) and Normal human astrocytes, cultured on porcine-derived brain extracellular matrix (ECM). The goal is to replicate the key features of the brain's microenvironment, enabling the cells to exhibit *in vivo*-like behavior within their native niche. This model will support the study of neuropathological diseases caused by pathogenic infections like *Toxoplasma gondii*.

Specific aim 1: Characterization of ECM components extracted from a porcine brain tissue.

Specific aim 2: Establishment of a 3D transwell *in vitro* model using human primary cell lines.

Specific aim 3: Elucidate the mechanism of *T. gondii* brain invasion.

CHAPTER IV

MATERIALS AND METHODS

A. CELL CULTURE

1. *ECVs-304 Cell Line*

ECVs-304 cells originate from human umbilical veins and exhibit features of both epithelial and endothelial cells. They share several common traits with endothelial cells and are commonly used in studies of cell-to-cell interaction, adhesion junctions, and angiogenesis (Xiong, 2011 #246). These cells are acquired from the American Type Culture Collection (ATCC), and cultured in Roswell Park Memorial Institute-1640 (RPMI-1640) (Sigma- Aldrich Life Science, Catalog # FBS-HI-12A, Germany), supplemented with 10% fetal bovine serum (FBS) (Capricorn Scientific, Germany), 1% penicillin/streptomycin (Biowest, p/s solution 100x, Catalog # L0022 100), and preserved in humidified incubator (37°C, 5% CO₂). The cells were passaged at 70-80% confluency using trypsin-EDTA (Sigma-Aldrich Life Science, Catalog# T4549, Germany).

2. *Human Aortic Endothelial Cells (HAECs)*

These endothelial cells, isolated from the human aorta, are considered a better replacement for ECVs in in vitro BBB studies because they share common morphological and functional properties of endothelial cells. Cells cryopreserved at passage 1, with 500,000 cells in each vial, were purchased from (Lonza, Switzerland). Cells were cultured in Vascular Cell Basal Medium (VCBM; ATCC, USA; CAT No. PCS-100-030) supplemented with FBS, penicillin and endothelial growth factors (ATCC, USA; Cat No. PCS100041). Maintained in a humidified incubator (37°C, 5% CO₂). The cells were

passaged at 70-80% confluency using trypsin-EDTA (Sigma Aldrich Life Science, Catalog# T4549, Germany). The subsequent experiments were conducted on HAECs of passages 4-6.

3. *Normal Human Astrocytes (NHAs)*

NHAs are primary astrocyte cells isolated from the human cerebral cortex. Given their critical role in maintaining BBB integrity, cellular organization in brain tissue, and their dynamic interaction with vascular endothelial cells, these cells are widely used in in vitro BBB studies. Cells are cryopreserved at passage 2 with 500,000 cells in each vial and are purchased from (iXCells Biotechnology, USA). These cells are cultured in astrocyte basal medium (iXCells Biotechnology, Catalog# MD-0039B, USA) supplemented with astrocyte growth supplement (iXCells Biotechnology, Catalog# MD-0039S, USA), fetal bovine serum (iXCells Biotechnology, Catalog# MD-0094, USA), and antibiotic-antimycotic (100X) (iXCells Biotechnology, Catalog# MD-0095, USA), and maintained in a humidified incubator (37°C, 5% CO₂). The cells are passaged at 70-80% confluency using trypsin-EDTA (Sigma-Aldrich Life Science, Catalog# T4549, Germany). The subsequent experiments were conducted on NHAs of passages 4-7.

4. *THP-1 CELLS*

THP-1 cells are a human monocytic cell line originally derived from a patient with acute monocytic leukemia. Given their expression of Toll-like receptors and secretion of inflammatory cytokines that closely mimic the responses of primary human monocytes, THP-1 cells serve as a valuable in vitro model for investigating the mechanisms of *Toxoplasma gondii* neuro-invasion. THP-1 cells are obtained from, and

maintained in Roswell Park Memorial Institute-1640 (RPMI-1640) (Sigma- Aldrich Life Science, Catalog # FBS-HI-12A, Germany), supplemented with 10% fetal bovine serum (FBS) (Capricorn Scientific, Germany), 1% penicillin/streptomycin (Biowest, p/s solution 100x, Catalog # L0022-100), and kept in a humidified incubator (37 °C. 5% CO₂). THP1 cells are cultured as suspension cells in a T25 or T75 flask and are passaged every 2-3 days to maintain a seeding density of 2x10⁶ cells

5. *Tachyzoites*

GFP-labelled Tachyzoites (RH-GFP 5S65T strain) were used in our model. Tachyzoites were serially passaged in human foreskin fibroblasts (HFFs) (American Type Culture Collection (ATCC)-CRL 1634) cultured in Dulbecco's Modified Eagle's Medium (DMEM) (GIBCO, Invitrogen) and supplemented with 10% fetal bovine serum (FBS), 1% penicillin-streptomycin, and 1% glutamine (SIGMA; Roedermark, Germany).

6. *Cell Viability and Proliferation Assay*

All cell lines were assessed daily using Zen software with a Zeiss Vert A1 microscope (Carl Zeiss AG, Germany), following up on any morphological changes and qualitative proliferation rates. Cells were seeded in 24-well plates at each line's specific seeding density.

Table 2: Seeding Density of Different Cell Lines Per cm²

Cell line	Seeding density per cm²
ECV-304	20,000

HAEC	20,000
NHA	6,000
THP-1	$2-5 \times 10^5$ cells/mL

B. Porcine Brain Extracellular Matrix

1. ECM Extraction

a. With Decellularization

Fresh pig brain tissue was preserved by lyophilization using a Labconco FreeZone 2.5L freeze dryer (Labconco Corp., USA) at -30°C under vacuum pressures below 0.1 mbar for 48 hours. Once dried, the tissue was ground into a fine powder for ECM extraction. The pulverized porcine brain was gradually added to a 3.4 M NaCl buffer containing protease inhibitor cocktail tablets (complete, Roche, Cat. No. 11697498001) and N-ethylmaleimide (Sigma-Aldrich Life Sciences, Cat. No. E3876-5G, Taufkirchen, Germany). The mixture was homogenized with Tissue Tear™ until it reached a milkshake-like consistency. This homogenate was centrifuged at 14,000g at 4°C for 1 hour. The process was repeated twice, discarding the supernatants and collecting the pellets each time.

The pellets were combined in a 4M urea buffer and homogenized again using the tissue terror at a lower power. The resulting homogenate were centrifuged at 14,000g for 1 hour at 4°C . the supernatant was then recuperated and exposed to several rounds, 2 hours each, of dialysis against a 0.9% NaCl, 50mM Tris supplemented with chloroform using a dialysis membrane tubing having a molecular wight cutoff of 6000-8000 Da (Spectrum Medical Industries, Spectra Por, Cat. No. 228716, LA, USA). The latter product was then dialyzed overnight at 4°C against RPMI-1640 (Sigma-Aldrich Life

Science, Catalog # FBS-HI-12A, Germany) with 1% penicillin-streptomycin. The final product was then aliquoted into 1.5ml volumes and stored at -80°C for later use.

b. Whole Brain Extract Extraction Protocol

0.5g of pulverized brain tissue was resuspended in 5ml of phosphate buffer saline (PBS 1X) and homogenized using Tissue Tearor™ until a uniform texture appeared. The homogenate was then centrifuged at 12,000g for 15 min, and the supernatant was collected. This process was repeated as necessary to remove residual debris. The product was filtered through a 0.2 µm syringe filter (Corning, catalog # 431219, Germany), and 1% penicillin/streptomycin (Biowest cat#L0022) was added.

2. ECM Protein Quantification

Following ECM extraction, protein content from both decellularized and non-decellularized brain tissues was measured by the DC protein assay kit (Bio-Rad Catalog #500-0113, Hercules, California, USA) according to the manufacturer's instructions. This assay is performed and assessed by comparison to a 2mg/ml Bovine Serum Albumin BSA standard solution provided by the kit manufacturer. The absorbance of these samples was measured at 750 nm using a multi-well spectrophotometer (Thermometer Scientific Multiskan EX, Thermometer Scientific USA).

3. SDS-Polyacrylamide Gel Electrophoresis SDS-PAGE for ECM Proteins

To separate proteins present in both ECM samples extracted according to their molecular weight, 10% polyacrylamide gels were prepared and loaded with 80µg of

samples, then run at 30mA in a sodium dodecyl-sulfate polyacrylamide gel electrophoresis (SDS-PAGE).

The resulting gel was stained overnight with Coomassie Blue stain and destained with high methanol solution, followed by low methanol solution until the background was reduced and clear bands appeared. Imaging was later performed on the Bio-Rad ChemiDoc MP system (1708280, BioRad, Hercules, CA., USA)

The efficiency of decellularization and preservation of ECM proteins was evaluated by comparing the protein band profiles of decellularized tissue to those of non-decellularized.

C. Proliferation Assay

To evaluate the viability and proliferation of HAECs under different concentrations of decellularized and non-decellularized brain ECM extracts, a proliferation assay was performed. ECM extracts at concentrations of 0.2 $\mu\text{g}/\mu\text{L}$ and 0.4 $\mu\text{g}/\mu\text{L}$ were prepared by diluting the extracts in cold, incomplete media (VCBM). HAECs were trypsinized, counted, and seeded at a density of 10,000 cells/cm² into 12-well plates containing the various ECM conditions. Cell viability and proliferation were assessed at 24-, 48-, and 72-hours post-seeding using Trypan Blue staining, followed by manual counting with a hemocytometer.

D. BBB Modelling

A three-dimensional (3D) in vitro model was developed using a transwell culture system. For the initial setup, 12-well transparent polyethylene terephthalate (PET) membrane cell culture inserts with a 0.4 μm pore size (Corning, USA) were chosen, as

they offer the most stable barrier resistance and optimal cell-cell contact. These inserts were used to assess barrier integrity through trans-epithelial/endothelial electric resistance (TEER), permeability assays, and immunofluorescence (IF). Inserts were either uncoated, coated with 10% Matrigel (100 $\mu\text{l}/\text{cm}^2$) (Corning®, cat#356230), or coated with 10% Matrigel supplemented with brain ECM at a concentration of 0.2 mg/ml. Notably, inserts coated with Matrigel and Brain ECM were incubated for an hour to allow gelation, after which excess Matrigel was removed, and HAECs were seeded on top.

1. Co-culture of HAEC and NHA

To better mimic the in vivo BBB, the use of human primary cells was essential. Two experimental conditions were established by utilizing 12 trans-well inserts in each batch. For the first condition, 12 trans-well inserts were seeded with a suspension of NHA in astrocyte media and 30% Matrigel with 0.2 mg/mL Brain ECM. After overnight incubation at 37 °C, Astrocyte Basal Medium was added to the apical and basal compartments, and embedded cells were allowed to reach approximately ~70% confluency, after which media from the apical side was removed and HAEC were seeded atop (11×10^3 cells) in endothelial basal media and were left to adhere. In the second condition, 12 trans-well inserts were seeded with a suspension of NHA in astrocyte media and 30% Matrigel with 0.2 mg/mL Brain ECM. Following overnight incubation at 37 °C, a 10% Matrigel coating was applied over the established membrane with embedded NHA. Astrocyte Basal Medium was again added to the apical and basal compartments. Once the cells had reached 70% confluency, media from the apical side was removed and HAEC were seeded atop (11×10^3 cells) in endothelial basal media and were left to adhere.

2. Matrigel and ECM Composite Thickness Assessment

As part of the co-culture model development, we aimed to determine the optimal concentration of a Matrigel and brain ECM composite that supports endothelial cell adhesion and monolayer formation without triggering angiogenesis. Given that 10% Matrigel alone was insufficient to embed normal human astrocytes (NHAs), we tested composite hydrogels composed of Matrigel at 10%, 20%, 30%, 40%, and 50% concentrations, each supplemented with 0.2 $\mu\text{g}/\mu\text{L}$ of decellularized brain ECM extract. HAECs were seeded on top of each composite, and their behavior was monitored over the following days. Samples were then fixed and stained with DAPI to evaluate cellular organization and matrix thickness. Confocal z-stack imaging was performed to measure the thickness of each composite and to identify conditions that allowed HAEC monolayer formation without signs of angiogenic sprouting.

E. Evaluation of Barrier Integrity and Functionality

1. TEER

Trans-epithelial/endothelial electrical resistance (TEER) was measured to assess the integrity of endothelial monolayers using an EVOM² voltmeter and STX3 electrodes (World Precision Instruments, Florida, USA). First, the Electrodes were sterilized in 70% ethanol and equilibrated in PBS (1X) for 10 minutes. Inserts (12-well, 0.4 μm pore size, 0.9 cm^2 surface area; Corning®, North Carolina, USA) were prepared by removing culture medium, gently washing twice with PBS, and adding 600 μL and 1.6 mL of PBS to the apical and basolateral compartments, respectively. Measurements were taken in triplicate for each insert. To calculate the final TEER result, the mean value was subtracted from the blank and multiplied by the surface area of the insert (cm^2).

2. Permeability Assay Evan's Blue (EB) and Sodium Fluorescein (NaF) permeability assay

Evans Blue (EB) of (MW=961 Da) is a fluorescent tracer that tightly binds to circulating plasma proteins, making its diffusion across a barrier a useful indicator of protein extravasation. In contrast, Sodium Fluorescein (NAF) of (MW=376 Da) is a small, low molecular weight dye that does not bind to plasma proteins and instead relies on its plasma concentration to permeate into the brain. Disruption of endothelial barrier integrity leads to increased permeability and passive leakage of these tracers into the basolateral compartment. Once a confluent endothelial monolayer was established on PET membrane inserts (pore size 0.4 μm ; Corning®, North Carolina, USA), EB was prepared at a concentration of 170 $\mu\text{g/ml}$ in 1% BSA (67 KDa; GIBCO®, Scotland), and NAF was added at 10 $\mu\text{g/ml}$. The solution was filtered using 0.22 μm syringe filters (Corning®, Germany). Before application, cells were washed twice with PBS. Then, 400 μl of the tracer solution was carefully added to the apical side (insert), while 1.5 ml of PBS was added to the lower chamber. Plates were incubated at 37°C, and every 30 minutes and for a total of 2 hours, 200 μl samples were collected from the basolateral compartment and replaced with fresh PBS. The optical densities were measured at 630 nm for EB and 492 nm for NaF, and the concentrations of the markers were calculated.

3. Monocytes Transmigration Assay

This assay was conducted to identify the in vitro model that exhibits the lowest rate of immune cell extravasation across the blood-brain barrier. For this assay, cells were seeded onto 12 inserts of 8 μm pore size and maintained under culture conditions till a confluent monolayer was established. On the day of the transmigration assay, THP-1 cells

were harvested and resuspended in an incomplete RPMI medium, then incubated for 1 hour at 37 °C. After that, 1×10^5 THP-1 cells were added to the upper chamber of each insert containing incomplete RPMI medium, while the lower chamber was filled with complete RPMI medium supplemented with 10% fetal bovine serum (FBS) to serve as a chemoattractant. The plates were incubated at 37 °C and 5% CO₂ in the humidified incubator for 12 hours. After incubation, the medium from the lower compartment was collected, and cells were counted.

F. Molecular Analysis and Junctional Protein Expression

1. Gene Expression Assessment by Quantitative Real-Time Polymerase Chain Reaction

a. RNA Extraction

Total RNA was isolated from confluent cell monolayers grown on 6-well plates and 6-well plate inserts of 0.4 µm pore size (Corning®, USA) using TRI Reagent® (Sigma, Germany), following the manufacturer's protocol. Cells were scraped and incubated in TRI Reagent® for 5 minutes to allow complete lysis. This reagent effectively disrupts cellular membranes and solubilizes cellular components while preserving RNA integrity through inhibition of RNase activity. Chloroform was added to the lysate to induce phase separation into three distinct phases, with RNA localized in the upper aqueous phase. The RNA-containing aqueous layer was carefully collected, and RNA was precipitated using 100% isopropanol, followed by a wash with 75% ethanol. The RNA pellet was then resuspended in 20 µl of RNase-free water. RNA concentration was determined by measuring absorbance at 260 nm, and purity was

assessed by calculating the A260/A280 ratio using a Nanodrop spectrophotometer (DS-11 series spectrophotometer-fluorometer; De Novix).

b. cDNA

2 μ g of total RNA extracted was reverse transcribed into complementary DNA (cDNA) using High-Capacity cDNA Reverse Transcription Kit as per manufacturer's instructions (Applied Biosystem, Thermofisher).

Quantified RNA samples were combined with 2 μ l of 10X RT buffer, 0.8 μ l of 25X dNTP mix, 2 μ l of 10X RT random primers, 1 μ l of reverse transcriptase, and 4.5 μ l of DEPC-treated water. To facilitate primer annealing to RNA sequence, samples were incubated at 25°C for 5 minutes, followed by the reverse transcription step at 46°C for 20 minutes using a thermal cycler (BioRad T100 thermal cycler, Hercules, CA, USA). The enzymatic activity was terminated by heating the samples at 95°C for 1 minute. The obtained samples were then stored at -80°C until further use.

c. Quantitative Real-Time Polymerase Chain Reaction (qRT-PCR)

A total of 2 μ g of cDNA was amplified using a homemade SYBR Green super mix containing dNTPs and Taq DNA polymerase. Reactions were prepared in duplicates using gene-specific forward and reverse primers on a BioRad CFX96 real-time PCR system. (see Table 3). Cycling condition starts with denaturation of dsDNA at 95°C for 3 minutes, followed by 40 amplification cycles (95°C denaturation for 30 seconds, annealing step for 30 seconds at the primers' annealing temperature, and extension at 72°C for 30 seconds) and a final extension cycle at 72°C for 5 minutes. The relative expression of target genes was calculated using the comparative $\Delta\Delta C_t$ method, with

human glyceraldehyde 3-phosphate dehydrogenase (GAPDH) serving as the internal reference gene for normalization.

Table 3: RT-qPCR Primer Sequences and Annealing Temperatures for the Studied Human Genes

Primers	Oligonucleotide Sequence	Annealing Temperature (°C)
GAPDH	F: TGG TGC TCA GTG TAG CCC AG R: GGA CCT GAC CTG CCG TCT AG	52-62
CLDN 5	F: CTGGACCACAACATCGTGA R: CACCGAGTCGTACACTTTGC	60
ZO-1	F: CAGCCGGTCACGATCTCCT R: TCCGGAGACTGCCATTGC	58
Cx43	F: CTT CAC TAC TTT TAA GCA AAA GAG R: TCC CTC CAG CAG TTG AG	

GAPDH: glyceraldehyde-3-phosphate dehydrogenase/ CLDN 5: claudin 5/ ZO-1: zona occluden 1/ Cx43: connexin-43

G. Immunofluorescence for Phenotypic Characterization and Adherent

Junctional Protein Localization

Cells were grown on 12 inserts and divided into 3 experimental groups: (1) HAECs seeded alone (control), (2) HAECs seeded on 10% Matrigel, and (3) HAECs seeded on 10% Matrigel combined with 0.2µg/µl of porcine brain ECM. Cells were maintained in culture until they formed a confluent monolayer. Following this, cells were washed twice with PBS and then fixed with 4% paraformaldehyde (PFA) for 25 minutes. Fixed Samples were then permeabilized using 0.1% Triton-X for 12 minutes and subsequently blocked with 5% BSA for one hour at RT. Samples were then incubated with primary antibodies (mouse anti-ZO-1 antibody and rabbit anti-CLDN-5 antibody)

overnight. The next day, membranes were washed and then labelled with a secondary antibody (Alexa Fluor 488 goat anti-mouse IgG and Texas Red goat anti-rabbit IgG). Nuclear staining was performed using a 1 $\mu\text{g}/\mu\text{L}$ 4,6-diamidino-2-phenylindole, Dihydrochloride (DAPI) solution. Finally, membranes were mounted using an aqueous antifade solution (Anti-Fade Fluorescence Mounting Medium).

Table 4: Antibodies Used for Immunofluorescence

Antibodies	Manufacturer	Probing
mouse anti-ZO-1	Invitrogen Catalog # 33-9100	Primary antibody
mouse anti-GFAP	Abcam Catalog # ab10062	Primary antibody
Rabbit anti-CLDN-5	Abcam Catalog #ab131259	Primary antibody
Alexa Fluor 488 goat anti-mouse	Life Technologies Catalog # A11001	Fluorescent secondary antibody
Texas Red goat anti-rabbit	Invitrogen Molecular Probes Catalog# T2767	Fluorescent secondary antibody

ZO-1: zona occluden 1/ CLDN-5: claudin-5/ GFAP: glial fibrillary acidic protein

H. Protein Extraction and Western Blot

Cells were washed with ice-cold PBS and scraped on ice in lysis buffer (0.5 M Tris-HCl buffer, pH 6.8; 2% SDS, and 20% glycerol) containing protease and phosphatase inhibitors, as well as ice-cold RIPA buffer (Roche, Basel, Switzerland). The cell lysate was collected and sonicated, then measured using the DC protein assay kit (Bio-Rad Catalog #500-0113, Hercules, California, USA). Protein samples were loaded onto 10% SDS-polyacrylamide gels and subjected to electrophoresis. Proteins were transferred to nitrocellulose membranes (BIO-RAD Cat# 162-0112; Hercules, CA, USA) at 30 V overnight using a BIO-RAD transfer unit. The next day, membranes were blocked with 5% non-fat milk powder dissolved in PBS 1X for 1 hour. Subsequently, membranes

were incubated with specific primary antibodies in blocking buffer for 3 hours at room temperature, then washed three times with PBS containing 0.1% Tween-20 and incubated with the corresponding HRP secondary antibodies in blocking buffer for 1 hour. After that, the membranes were washed again with PBS-0.1% Tween-20 before visualizing the protein bands on the ChemiDoc system. Band quantification was performed using ImageJ software.

I. T. gondii Invasion Assay

1. Effect of Tachyzoite Infection on the Transmigration of Monocytes Through an Endothelial Barrier

To study the effect of tachyzoite infection on the transmigration rate of THP-1 cells across an endothelial barrier, endothelial cells were seeded on a pre-coated 12-well insert (8 μm pore size; Corning®, USA) and divided into 2 groups: confluent endothelial monolayers and leaky non-confluent monolayers. Each condition was further divided into 2 subgroups: THP-1 control cells and THP-1 cells pre-infected with tachyzoites for 6 hours before seeding.

Before adding THP-1 cells, the inserts were gently washed with PBS, followed by the addition of serum-free RPMI medium to the apical compartment, and complete RPMI medium supplemented with 10% FBS was added to the lower compartment. A total of 1×10^5 cells from each group was seeded into their respective inserts and incubated for 12 hours in a humidified chamber. After incubation, media from the lower chamber were collected, and the number of extravasating cells was counted using Trypan Blue assay.

2. Live Cell Imaging of Tachyzoites Co-Cultured with THP-1 Cells on an Endothelial Barrier

Live cell imaging was performed to observe the interaction, behavior, and dissemination routes of tachyzoites when co-cultured with THP-1 cells on an in vitro endothelial barrier. Cells were seeded on a 12-well insert of (8 μm pore size; Corning®, USA) pre-coated with 10% Matrigel supplemented with 0.2 mg/mL Brain ECM. Cells were maintained in a humidified incubator (at 37 °C and 5% CO₂) till a confluent endothelial monolayer was formed. On the day of live imaging, Endothelial media was removed, washed with PBS, and serum-free RPMI medium was added to the apical compartment of the insert. A suspension containing an equal number of THP-1 cells and RHHX strain tachyzoites (of final seeding density 1×10^5 cells/ cm^2) was added to the insert of the endothelial monolayer. The insert was then placed in a well of a glass-bottomed confocal dish containing complete RPMI medium supplemented with 10% FBS to establish a chemotactic gradient.

The inserts were then placed on a heated microscope stage with a live-cell incubation chamber maintained at 37 °C and 5% CO₂. Imaging was conducted with a laser scanning confocal microscope (LSM 710, Carl Zeiss, Germany) controlled by Zeiss LSM 710 software. Time-series imaging was performed by acquiring one image every 5 minutes for 132 cycles, generating a 12-hour video. Visualization of the cells was achieved using the FITC channel to detect GFP-labelled tachyzoites, while the transmitted light (T-PMT) mode was used to observe the underlying endothelial monolayer and unlabeled, circular THP-1 cells. Imaging was carried out using a 20x objective lens.

To further evaluate tachyzoites' extravasation, Z-stack imaging was performed before and after time-lapse recording through the full thickness of the membrane. This allowed the comparison of the parasite localization and transmigration in three dimensions after 12 hours of incubation on an endothelial barrier.

J. Drug Screening

Live/Dead Assay to Evaluate Imiquimod Cytotoxicity on HAEC

A Live/Dead assay was performed to assess whether the imiquimod drug has a cytotoxic effect on endothelial cells. Cells were seeded onto pre-coated 24-well inserts (0.4 μm pore size; Corning, USA) and cultured until a confluent monolayer formed. Once the endothelial barrier was established, 10 μL of the drug (1 μM concentration) was added to the apical compartments containing VCBM, and the plate was incubated at 37 °C with 5% CO_2 for 48 hours. Afterward, media from both the lower and upper compartments were removed, gently washed with PBS, and incubated for 1 hour with Calcein-AM (for live cells) and Propidium Iodide (PI) (for dead cells) at 37 °C. Following this, the inserts were washed with PBS and fixed with 4% PFA for 25 minutes, then mounted on glass slides using an aqueous antifade solution for fluorescent imaging.

CHAPTER V

RESULTS

A. Optimization of the Blood-Brain Barrier In Vitro Model Using ECV-304 Cell Line

For the optimization process, TEER and permeability assays were conducted on ECV-304 (control group) and ECV-304 (seeded on 10% Matrigel), and the results highlight a significant increase in TEER value and a major reduction in Evans' Blue permeability in the condition of cells seeded on 10% Matrigel.

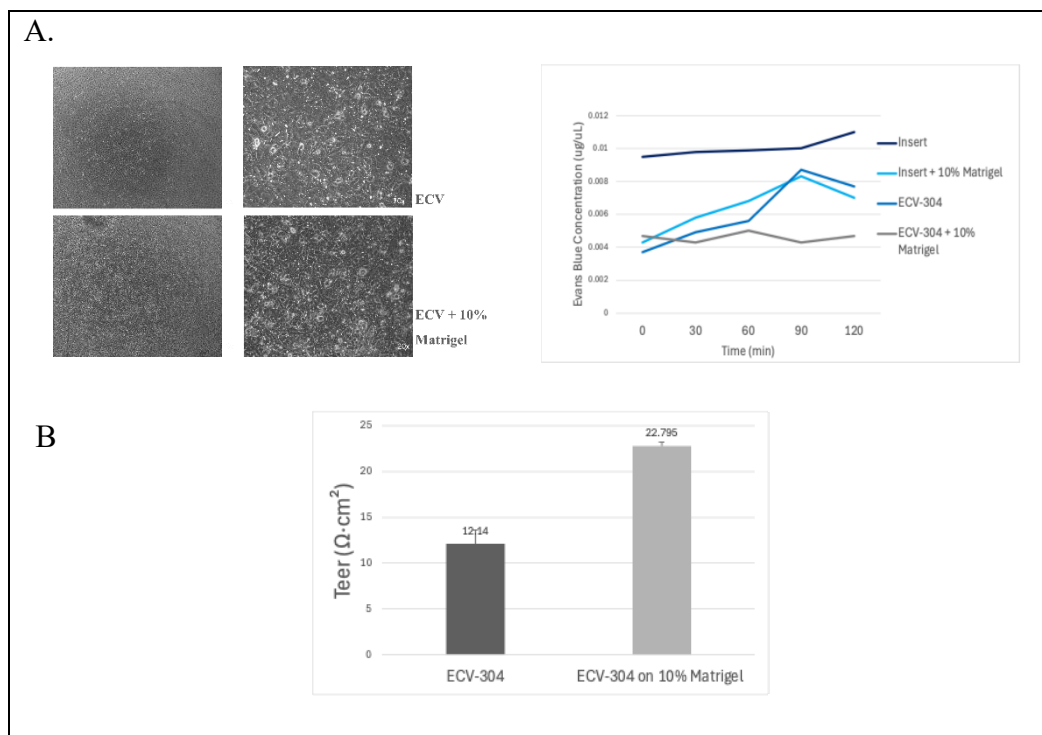


Figure 5: Optimization of in Vitro BBB Using ECV-304 Cell Line

(A) Light microscopy images of ECV-304 forming a monolayer in both control and Matrigel conditions before conducting TEER and Permeability assays. (B) Evans' Blue permeability assay, where the level of molecules that crossed the membrane was measured by spectrophotometry and plotted as means over time. (C) Bar graphs indicate average TEER measurements of different cell culture conditions.

B. Importance of Using Human Primary Cells for the *In Vitro* BBB Model:

Immunofluorescence conducted on ECV-304 seeded on top of NHA embedded in 50% Matrigel showed that cells co-cultured with NHAs have an intensified expression of TJ proteins like ZO-1 than ECV-304 seeded alone.

In another assay, Immunofluorescence was done on monolayers of ECV-304 and a Monolayer of HAEC, both seeded on top of 10% Matrigel, to compare the expression of CD31 endothelial cell marker. The result revealed that HAECs exhibited a stronger and more localized expression CD31 endothelial marker than ECV-304.

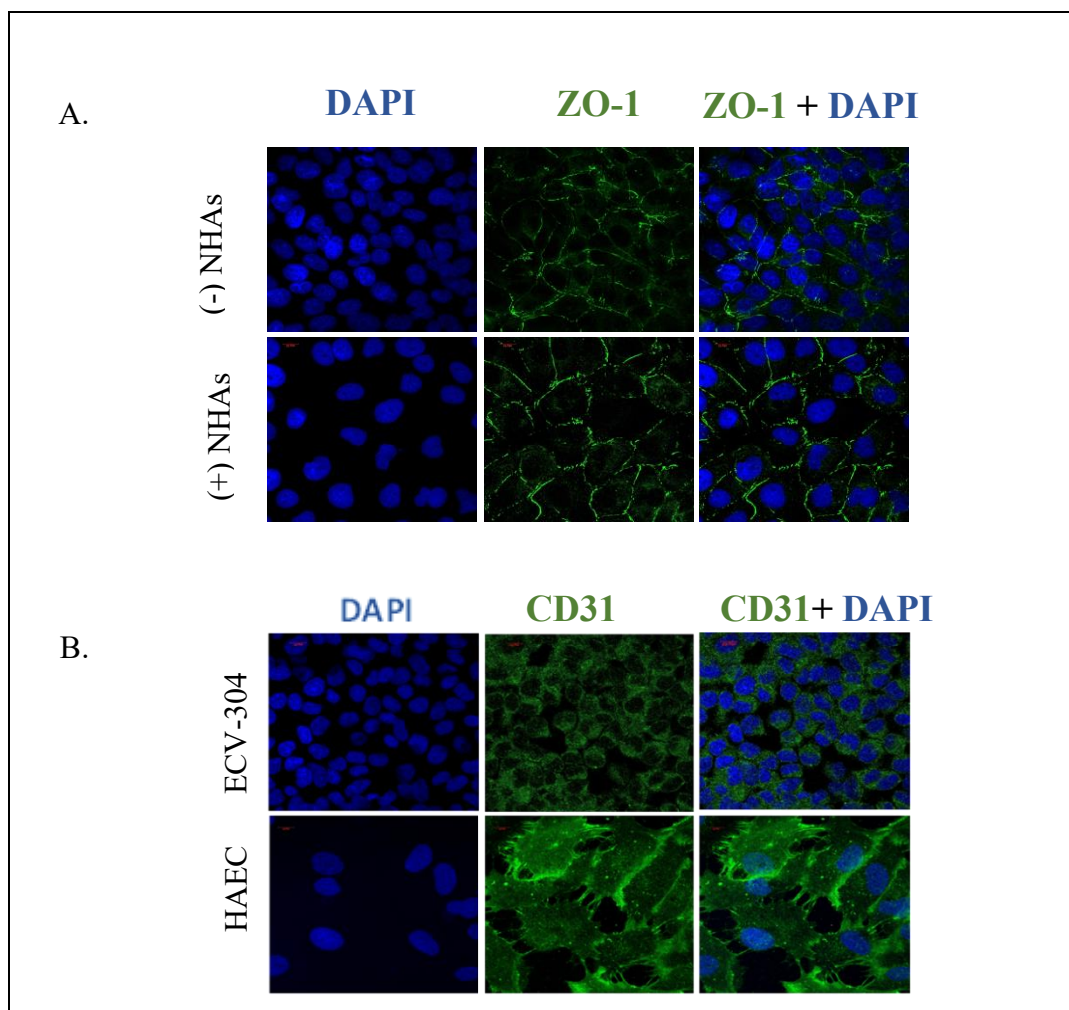


Figure 6: Immunofluorescence Images of 63X Magnification

(A) Immunofluorescence images of ECV-304 with and without NHAs, stained for ZO-1 TJ protein. (B) Immunofluorescence for the CD31 marker on ECV-304 cells and HAEC.

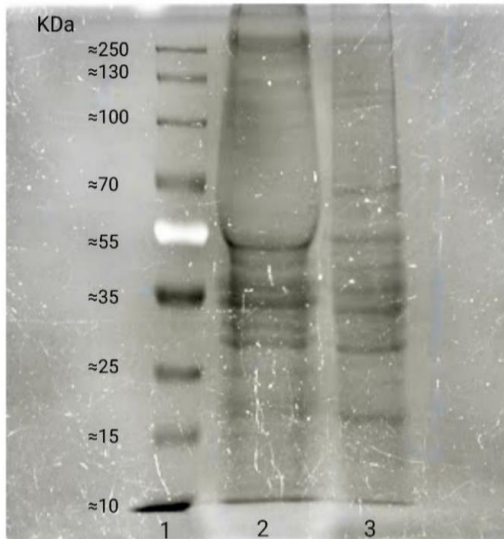
C. Characterization of ECM Extracted from Porcine Brain Tissue and ECM

Dose Response on HAECs

After extracting ECM from porcine brain tissue using two methods: decellularization and non-decellularization, we analyzed their protein compositions using SDS-PAGE. The gel result indicates that a broad array of ECM proteins was retained in both samples, showing a small bulge and thicker bands in the decellularized extract, with no significant loss of protein.

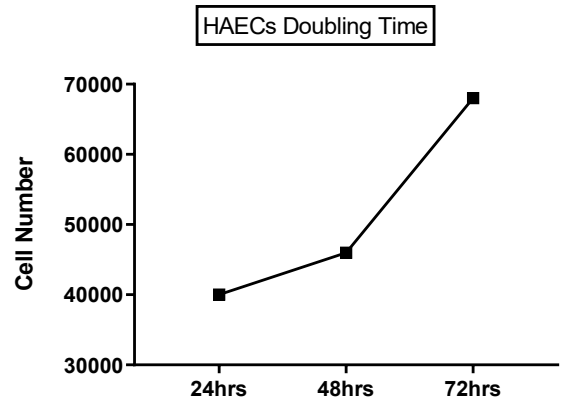
After that, HAEC were seeded on different concentrations of both ECM extracts. A trypan blue exclusion assay was performed at 24, 48, and 72 hours. Cell counts and light microscopy images revealed that 0.2 μ g/ μ l of decellularized ECM proteins displays the highest cell proliferation rate and cell viability than the other conditions.

A.

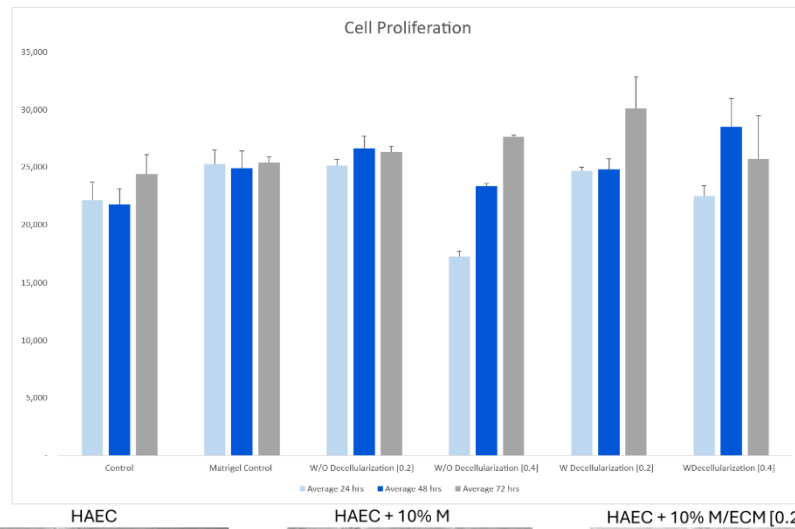


B.

Time	24 hours	48 hours	72 hours
Cell Number	40,000	46,000	68,000



C.



D.

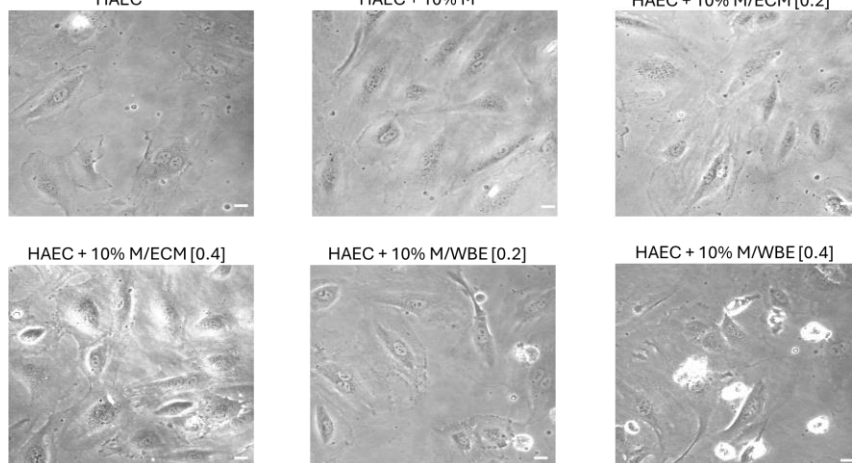


Figure 7: ECM Extraction Analysis and Dose Response

(A) SDS-PAGE analysis of ECM extracted from a porcine brain tissue: (Lane 1): Protein Ladder, (Lane 2): ECM extract from a decellularized brain tissue, (Lane 3): ECM extract

from a non-decellularized brain tissue. (B) Bar graph corresponding to HAEC doubling time. (C) cell proliferation rate of HAECs under different concentrations of ECM extracts (WO: without / W: with). (D) Light microscopy images of HAECs after 72 hours of incubation with Various doses of ECM extracts (scale bar: 200 μ m).

D. Modeling the Endothelial Monolayer with HAEC

1. Functional Assays

TEER and Permeability assays were conducted on HAEC of different culture groups. The results showed that cells seeded on Matrigel + ECM extract exhibit the highest TEER values, lowest permeability to molecular tracers like (EB) and (NaF), and a significant reduction in THP-1 cells transmigration. Furthermore, Immunofluorescence was performed to localize adherent junction proteins like ZO-1 and CLDN-5, which revealed an improved expression pattern of these TJ proteins under this culture condition as well.

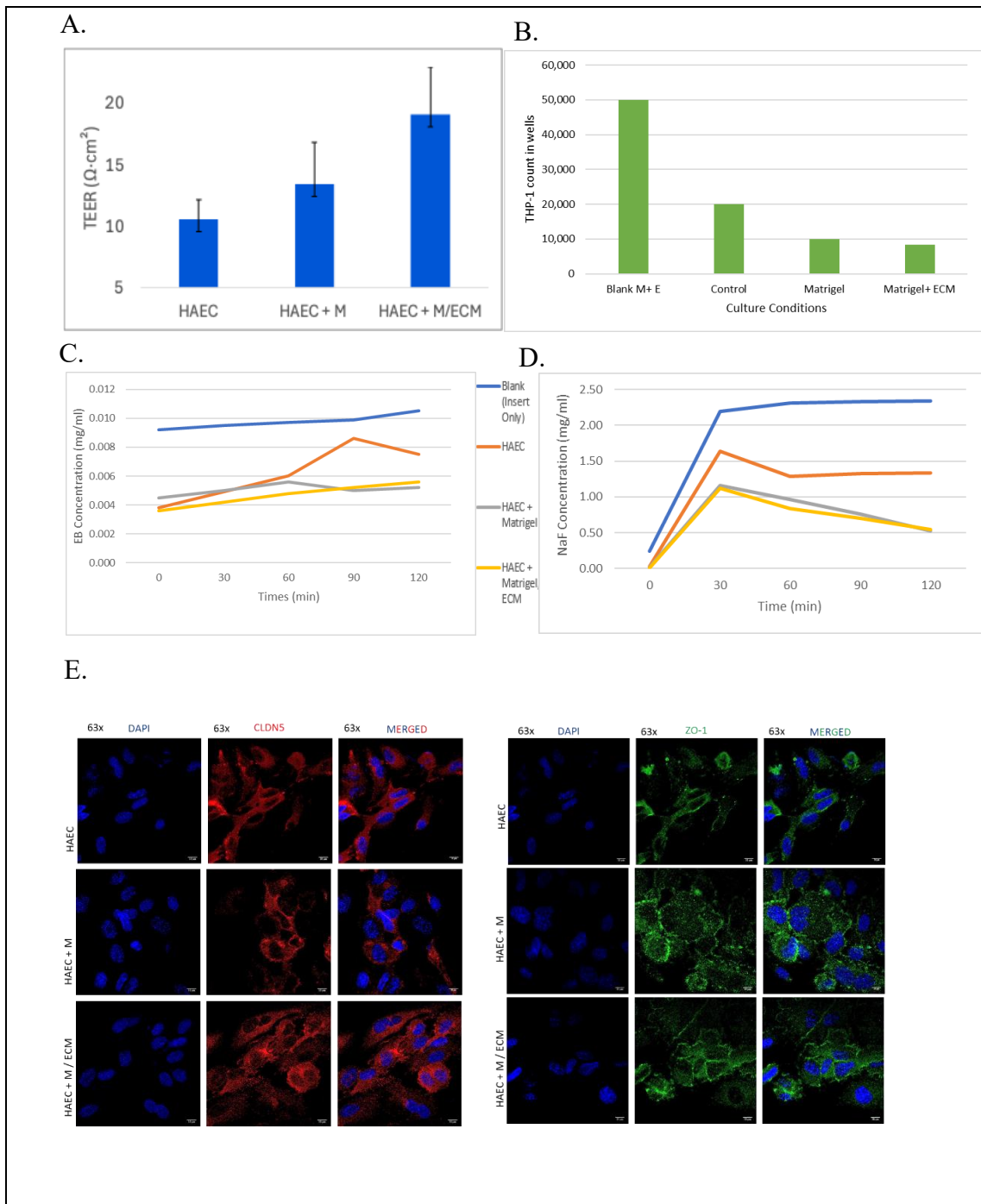


Figure 8: Functional Assays Analysis of HAECs

(A) Bar graphs indicate average TEER measurements of the barrier integrity. (B) Bar graph showing THP-1 cells transmigration assay. Membrane permeability was evaluated by (C) Evans' Blue and (D) Sodium Fluorescein molecular tracers. (E) Immunofluorescence images of HAECs to assess expression and localization of adherent junction proteins ZO-1 and CLDN-5 (scale bar: 10 μm).

2. Molecular Assays

Cells were seeded into 3 different groups as mentioned before: control, Matrigel, and Matrigel+ ECM for qRT-PCR and Western Blot analysis of ZO-1 and CLDN-5 proteins. Results showed an elevated expression of CLDN-5 protein in the condition of Matrigel combined with ECM, whereas, for ZO-1 protein, this expression was elevated more in the condition of Matrigel alone. Similar results were obtained in qRT-PCR.

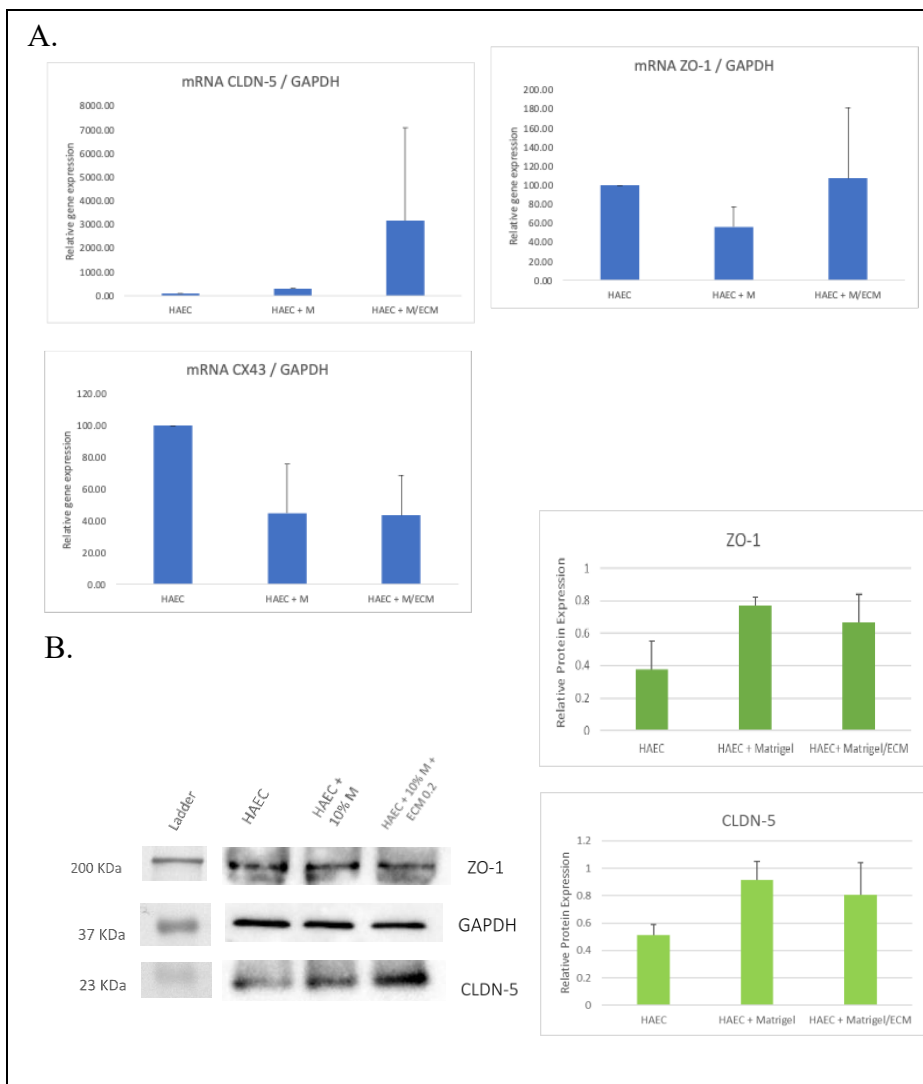


Figure 9: Molecular Assays Analysis of ZO-1, Cx43, and CLDN-5 in HAECs

(A)qRT-PCR analysis showing relative mRNA expression levels of CLDN-5, ZO-1, and Cx43 in control, 10% Matrigel, and 10% Matrigel + 0.2 $\mu\text{g}/\mu\text{l}$ of ECM protein extract.

(B) Bar graph demonstrating relative protein expression of ZO-1 and CLDN-5 proteins. Expression levels were measured and normalized to GAPDH using ImageJ software. Results are presented as means \pm SEM with 2N samples.

E. Normal Human Astrocytes Maintenance and Co-culture

Light microscopy images revealed that only 10%, 20%, and 30% Matrigel concentrations did not induce capillary-like structure in HAECs, with respective gel thicknesses of 16 μ m, 18 μ m, and 20 μ m. Subsequently, the HAECs that were seeded on 30 % Matrigel still formed capillary tube-like structures when co-cultured with NHA embedded in 30% Matrigel. In another assay, NHAs were embedded in 30% Matrigel with 0.2 μ g/ μ l ECM, and HAECs were seeded on top with 10% Matrigel; however, no angiogenesis was observed, and HAECs formed a monolayer on top of NHAs.

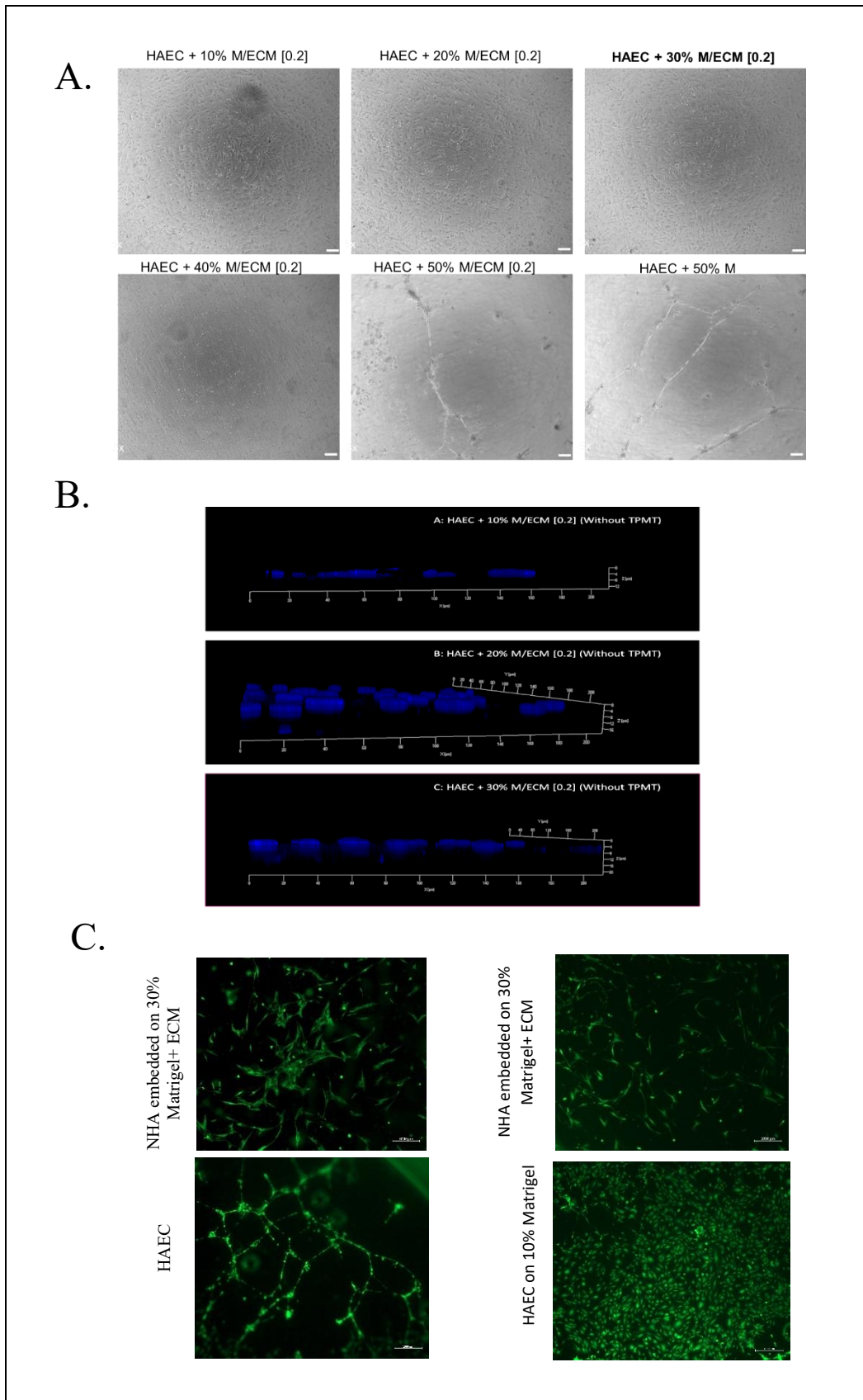


Figure 10: Optimization of Matrigel Concentration for co-culture of HAECs and NHAs (A) Light microscopy images of HAECs on different concentrations of Matrigel (scale bar: 200 μ m). (B) Corresponding Z-stack images of HAECs on 10%, 20%, and 30% Matrigel supplemented with 0.2 μ g/ μ l of ECM extract. (C) Immunofluorescence for Calcein-AM to present HAECs and NHAs in both culture conditions: with and without

10% Matrigel on top of NHAs in 30% Matrigel and 0.2 μ g/ μ l ECM extract (10X magnification).

F. T. gondii Dissemination Through an Endothelial Barrier

Immunofluorescence analysis in HFFs confirmed successful infection and robust GFP expression in tachyzoites of the type I (RHHX strain). In addition, transmigration assay of THP-1 across the endothelial barrier demonstrated a significantly higher extravasation in pre-infected THP-1 cells compared to the control group. Furthermore, live imaging of tachyzoites co-cultured with THP-1 on a HAECs monolayer showed a prominent display of transcellular and Trojan Horse pathways after 12 hours of incubation.

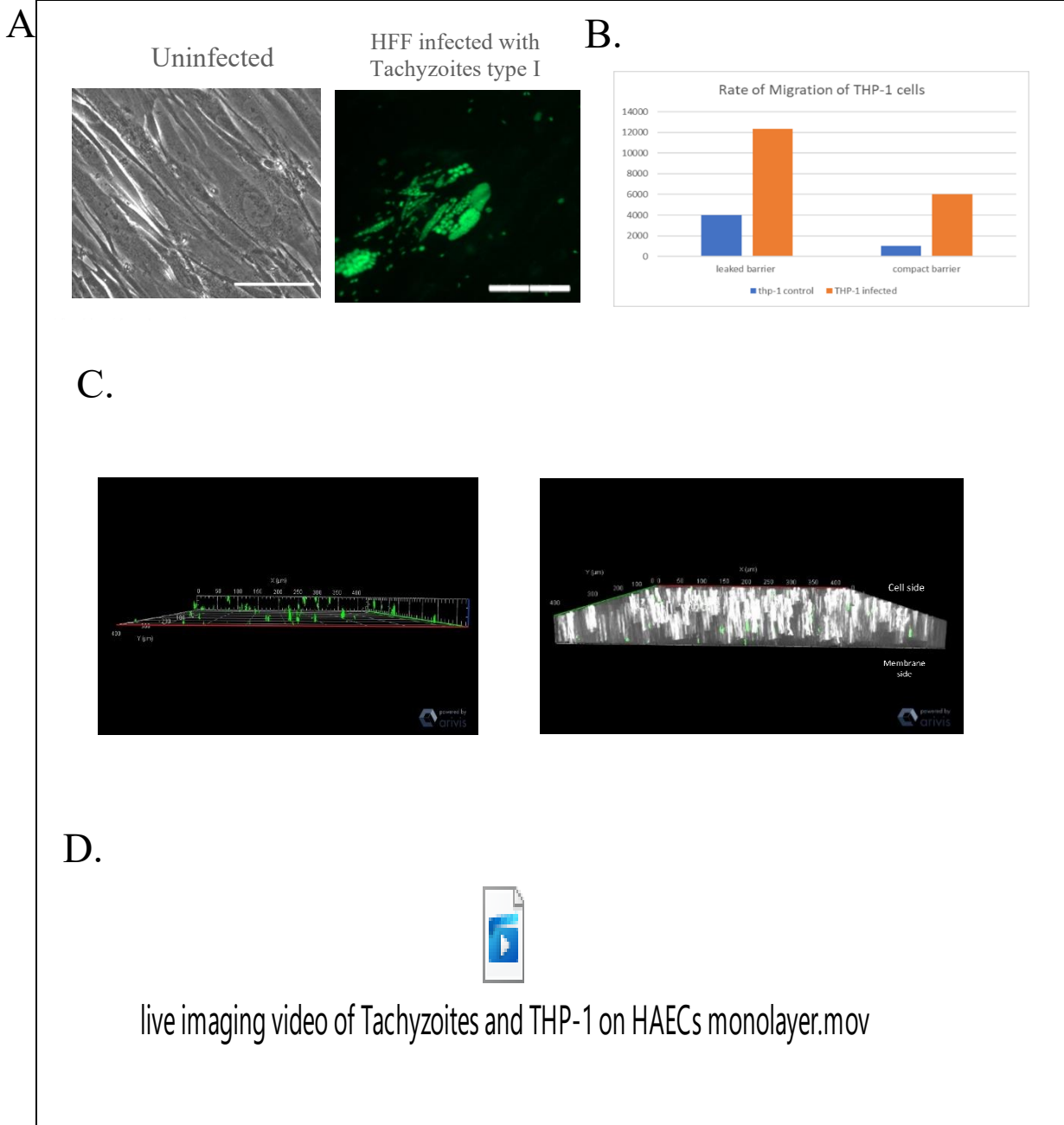


Figure 11: Tachyzoites Type I (RHHX strain) Extravasating Through the HAECs Monolayer

(A) Light and immunofluorescent images of HFFs infected and uninfected with GFP-labelled tachyzoites (scale bar: 200 μ m) (B) Bar graph showing the rate of THP-1 transmigration in the control and THP-1-infected groups. (C) Z-stack images of extravasating tachyzoite (D) Live-Cell Imaging of GFP labelled Tachyzoites co-cultured with THP-1 cells (small circular cells) on Endothelial Monolayer (displayed in T-PMT) using Zeiss LSM 710 software.

G. Testing the Effect of Imiquimod Drug on HAEC Monolayer

Live/Dead assay on HAEC treated with 1 μ M of imiquimod drug revealed no significant change in HAEC viability following 48 hours of treatment, compared to HAEC uninfected. However, it caused a slight change in cell morphology and count

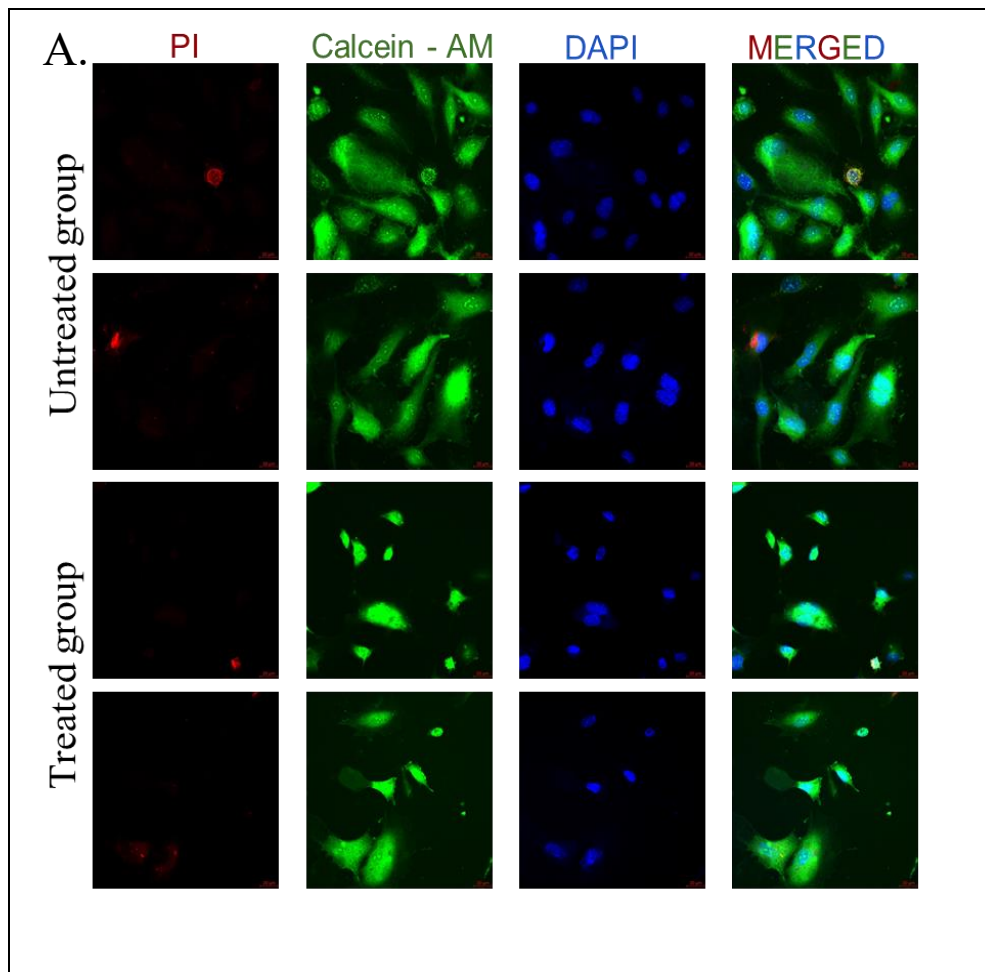


Figure 12: Live/Dead Assay of HAEC Treated and Untreated with Imiquimod

(A) Immunofluorescence images of HAECs stained with Calcein-AM and Propidium Iodide (PI) in treated and untreated conditions (scale bar: 20 μ m).

CHAPTER VI

DISCUSSION

In our project, we successfully established a novel *in vitro* human blood-brain barrier (BBB) model by culturing primary human cell lines within a porcine brain extracellular matrix (ECM-Matrigel composite). This approach aimed to recapitulate the biostructure properties of the brain's microenvironment by enabling the cells to adopt more physiologically relevant, *in vivo*-like behavior.

Characterization of the extracted ECM through SDS-PAGE revealed that the protein content was greatly preserved after decellularization, as evidenced by comparable protein band profiles between decellularized and whole-brain tissue samples, with slightly intense bands in the decellularized extract. This preservation was functionally confirmed in a dose-response assay, where cells exhibited nearly similar proliferation rates across different concentrations of decellularized and non-decellularized brain extracts. Notably, the highest proliferation rate and most favorable cell morphology were observed at 0.2 $\mu\text{g}/\mu\text{L}$ of decellularized ECM, which was selected for later experiments.

Importantly, the ECM–Matrigel composite significantly elevated trans-endothelial electrical resistance (TEER) values compared to control inserts, reflecting enhanced barrier integrity. This observation is aligned with previous reports showing that ECM components such as collagen IV, fibronectin, and nidogen contribute to increased resistance across endothelial monolayers [79]. The functional enhancement of the barrier was further supported by a corresponding reduction in permeability to molecular tracers (EB and NaF), as well as a reduction in the transmigration of immune cells, such as monocytes [80]. These findings were accompanied by a significant upregulation of ZO-

1 and CLDN-5 protein levels in the Matrigel-ECM conditions, with almost similar expression to that of Matrigel.

Our model also enabled us to perform real-time live-cell imaging to study *Toxoplasma gondii* interaction with our human in vitro endothelial barrier. The imaging revealed that tachyzoites utilize both the transcellular and "Trojan horse" mechanisms for crossing the barrier, with a marked predominance of the latter. This was also demonstrated by the increased transmigration rate of infected THP-1 monocytes compared to non-infected controls, consistent with findings by [81] on retinal endothelium. Moreover, infected monocytes displayed greater motility, increased adherence to the HAEC monolayer, and extended pseudopodia, further supporting their active involvement in facilitating parasite dissemination.

A preliminary cytotoxicity assessment on HAEC showed minor morphological changes after 48 hours of treatment. However, as these findings are based on a single replicate, further experimentation is needed to confirm efficacy and cytotoxicity.

Despite these promising outcomes, it is important to mention some of the difficulties that we faced during our work. Some of our assays were done as one set of experiments, which need further sets to strengthen our hypothesis. Another limitation was the absence of key NVU cell types, such as astrocytes, pericytes, and microglia, which are essential for replicating a physiologically relevant in vitro model. Additionally, technical difficulties, including the unexpected loss of our normal human astrocyte stock and delays in the ECM extraction process, limited the scope of experiments, particularly those involving therapeutic drug screening. Therefore, addressing these limitations in future work will be essential to improve the functionality of the in vitro BBB model.

In conclusion, the blood-brain barrier plays an essential role in preserving central nervous system (CNS) homeostasis by preventing the uncontrolled entry of pathogens, toxins, and malignant cells into the brain. Under pathological conditions such as pathological infection, inflammation, or cancer metastasis, this barrier becomes compromised, potentially contributing to disease progression. Developing robust in vitro BBB models that closely mimic the in vivo environment is necessary. Such models offer powerful tools for investigating neuropathological mechanisms, screening potential therapeutics, and reducing reliance on classical animal models.

REFERENCES

1. Abbott, N.J., et al., *Structure and function of the blood–brain barrier*. *Neurobiology of Disease*, 2010. **37**(1): p. 13-25.
2. Harilal, S., et al., *Revisiting the blood-brain barrier: A hard nut to crack in the transportation of drug molecules*. *Brain Res Bull*, 2020. **160**: p. 121-140.
3. Keaney, J. and M. Campbell, *The dynamic blood-brain barrier*. *Febs j*, 2015. **282**(21): p. 4067-79.
4. Tietz, S. and B. Engelhardt, *Brain barriers: Crosstalk between complex tight junctions and adherens junctions*. *J Cell Biol*, 2015. **209**(4): p. 493-506.
5. Obermeier, B., R. Daneman, and R.M. Ransohoff, *Development, maintenance and disruption of the blood-brain barrier*. *Nat Med*, 2013. **19**(12): p. 1584-96.
6. Nance, E., et al., *Drug delivery to the central nervous system*. *Nat Rev Mater*, 2022. **7**(4): p. 314-331.
7. Graham, A.K., et al., *Toxoplasmosis of the central nervous system: Manifestations vary with immune responses*. *Journal of the Neurological Sciences*, 2021. **420**.
8. Elsheikha, H.M., C.M. Marra, and X.Q. Zhu, *Epidemiology, Pathophysiology, Diagnosis, and Management of Cerebral Toxoplasmosis*. *Clin Microbiol Rev*, 2021. **34**(1).
9. Daher, D., et al., *Comprehensive Overview of Toxoplasma gondii-Induced and Associated Diseases*. *Pathogens*, 2021. **10**(11): p. 1351.
10. Virus, M.A., et al., *Neurological and Neurobehavioral Disorders Associated with Toxoplasma gondii Infection in Humans*. *J Parasitol Res*, 2021. **2021**: p. 6634807.
11. Mendez, O.A. and A.A. Koshy, *Toxoplasma gondii: Entry, association, and physiological influence on the central nervous system*. *PLoS Pathog*, 2017. **13**(7): p. e1006351.
12. Sivandzade, F. and L. Cucullo, *In-vitro blood-brain barrier modeling: A review of modern and fast-advancing technologies*. *J Cereb Blood Flow Metab*, 2018. **38**(10): p. 1667-1681.
13. Engelhardt, B., P. Vajkoczy, and R.O. Weller, *The movers and shapers in immune privilege of the CNS*. *Nature Immunology*, 2017. **18**(2): p. 123-131.
14. Ross, E.C., G.C. Olivera, and A. Barragan, *Early passage of *Toxoplasma gondii* across the blood–brain barrier*. *Trends in Parasitology*, 2022. **38**(6): p. 450-461.
15. Betsholtz, C., et al., *Advances and controversies in meningeal biology*. *Nature Neuroscience*, 2024.
16. McConnell, H.L. and A. Mishra, *Cells of the Blood-Brain Barrier: An Overview of the Neurovascular Unit in Health and Disease*. *Methods Mol Biol*, 2022. **2492**: p. 3-24.
17. Wu, D., et al., *The blood–brain barrier: Structure, regulation and drug delivery*. *Signal Transduction and Targeted Therapy*, 2023. **8**(1): p. 217.
18. Correale, J. and A. Villa, *Cellular Elements of the Blood-Brain Barrier*. *Neurochemical Research*, 2009. **34**(12): p. 2067-2077.
19. Persidsky, Y., et al., *Blood–brain Barrier: Structural Components and Function Under Physiologic and Pathologic Conditions*. *Journal of Neuroimmune Pharmacology*, 2006. **1**(3): p. 223-236.
20. Jamieson, J.J., P.C. Searson, and S. Gerecht, *Engineering the human blood-brain barrier in vitro*. *Journal of Biological Engineering*, 2017. **11**(1): p. 37.

21. Lippmann, E.S., et al., *Derivation of blood-brain barrier endothelial cells from human pluripotent stem cells*. Nat Biotechnol, 2012. **30**(8): p. 783-91.
22. Villaseñor, R., et al., *Intracellular transport and regulation of transcytosis across the blood-brain barrier*. Cell Mol Life Sci, 2019. **76**(6): p. 1081-1092.
23. Galea, I., *The blood–brain barrier in systemic infection and inflammation*. Cellular & Molecular Immunology, 2021. **18**(11): p. 2489-2501.
24. Dancy, C., K.E. Heintzelman, and M.E. Katt, *The Glycocalyx: The Importance of Sugar Coating the Blood-Brain Barrier*. Int J Mol Sci, 2024. **25**(15).
25. Willis, C.L., et al., *Focal astrocyte loss is followed by microvascular damage, with subsequent repair of the blood-brain barrier in the apparent absence of direct astrocytic contact*. Glia, 2004. **45**(4): p. 325-337.
26. Allen, N.J. and D.A. Lyons, *Glia as architects of central nervous system formation and function*. Science, 2018. **362**(6411): p. 181-185.
27. Galea, I., *The blood-brain barrier in systemic infection and inflammation*. Cell Mol Immunol, 2021. **18**(11): p. 2489-2501.
28. Vandebroek, A. and M. Yasui, *Regulation of AQP4 in the Central Nervous System*. Int J Mol Sci, 2020. **21**(5).
29. Stern, J.E., et al., *Astrocytes Contribute to Angiotensin II Stimulation of Hypothalamic Neuronal Activity and Sympathetic Outflow*. Hypertension, 2016. **68**(6): p. 1483-1493.
30. Sofroniew, M.V. and H.V. Vinters, *Astrocytes: biology and pathology*. Acta Neuropathol, 2010. **119**(1): p. 7-35.
31. Ronaldson, P.T. and T.P. Davis, *Blood-brain barrier integrity and glial support: mechanisms that can be targeted for novel therapeutic approaches in stroke*. Curr Pharm Des, 2012. **18**(25): p. 3624-44.
32. Török, O., et al., *Pericytes regulate vascular immune homeostasis in the CNS*. Proc Natl Acad Sci U S A, 2021. **118**(10).
33. Thomsen, M.S., L.J. Routhe, and T. Moos, *The vascular basement membrane in the healthy and pathological brain*. J Cereb Blood Flow Metab, 2017. **37**(10): p. 3300-3317.
34. Correale, J. and A. Villa, *Cellular elements of the blood-brain barrier*. Neurochem Res, 2009. **34**(12): p. 2067-77.
35. Alahmari, A., *Blood-Brain Barrier Overview: Structural and Functional Correlation*. Neural Plast, 2021. **2021**: p. 6564585.
36. Saliba, J., et al., *A Biomimetic Human Multi-Cellular In Vitro Model of the Blood-Brain Barrier*. Int J Mol Sci, 2025. **26**(8).
37. Wolburg, H. and A. Lippoldt, *Tight junctions of the blood–brain barrier: development, composition and regulation*. Vascular pharmacology, 2002. **38**(6): p. 323-337.
38. Günzel, D. and A.S. Yu, *Claudins and the modulation of tight junction permeability*. Physiol Rev, 2013. **93**(2): p. 525-69.
39. Hajal, C., et al., *Engineered human blood-brain barrier microfluidic model for vascular permeability analyses*. Nat Protoc, 2022. **17**(1): p. 95-128.
40. Alajangi, H.K., et al., *Blood–brain barrier: emerging trends on transport models and new-age strategies for therapeutics intervention against neurological disorders*. Molecular Brain, 2022. **15**(1): p. 49.
41. Abbott, N.J., et al., *Structure and function of the blood-brain barrier*. Neurobiol Dis, 2010. **37**(1): p. 13-25.

42. Tashima, T., *Smart Strategies for Therapeutic Agent Delivery into Brain across the Blood-Brain Barrier Using Receptor-Mediated Transcytosis*. Chem Pharm Bull (Tokyo), 2020. **68**(4): p. 316-325.
43. Nance, E., et al., *Drug delivery to the central nervous system*. Nature Reviews Materials, 2022. **7**(4): p. 314-331.
44. Niazi, S.K., *Non-Invasive Drug Delivery across the Blood-Brain Barrier: A Prospective Analysis*. Pharmaceutics, 2023. **15**(11).
45. Wu, D., et al., *The blood-brain barrier: structure, regulation, and drug delivery*. Signal Transduct Target Ther, 2023. **8**(1): p. 217.
46. Hersh, D.S., et al., *Evolving Drug Delivery Strategies to Overcome the Blood Brain Barrier*. Curr Pharm Des, 2016. **22**(9): p. 1177-1193.
47. Kim, S.-S., et al., *Effective treatment of glioblastoma requires crossing the blood–brain barrier and targeting tumors including cancer stem cells: The promise of nanomedicine*. Biochemical and Biophysical Research Communications, 2015. **468**(3): p. 485-489.
48. Bonhomme, A., L. Pingret, and J.M. Pinon, *Review: Toxoplasma gondii cellular invasion*. Parasitologia, 1992. **34**(1-3): p. 31-43.
49. Sanchez, S.G. and S. Besteiro, *The pathogenicity and virulence of Toxoplasma gondii*. Virulence, 2021. **12**(1): p. 3095-3114.
50. Skariah, S., M.K. McIntyre, and D.G. Mordue, *Toxoplasma gondii: determinants of tachyzoite to bradyzoite conversion*. Parasitol Res, 2010. **107**(2): p. 253-60.
51. E, S.A.-M., *Toxoplasmosis: stages of the protozoan life cycle and risk assessment in humans and animals for an enhanced awareness and an improved socio-economic status*. Saudi J Biol Sci, 2021. **28**(1): p. 962-969.
52. Hill, D. and J.P. Dubey, *Toxoplasma gondii: transmission, diagnosis and prevention*. Clin Microbiol Infect, 2002. **8**(10): p. 634-40.
53. Dubey, J.P., D.S. Lindsay, and C.A. Speer, *Structures of Toxoplasma gondii tachyzoites, bradyzoites, and sporozoites and biology and development of tissue cysts*. Clin Microbiol Rev, 1998. **11**(2): p. 267-99.
54. Wang, Z.D., et al., *Toxoplasma gondii Infection in Immunocompromised Patients: A Systematic Review and Meta-Analysis*. Front Microbiol, 2017. **8**: p. 389.
55. Feustel, S.M., M. Meissner, and O. Liesenfeld, *Toxoplasma gondii and the blood-brain barrier*. Virulence, 2012. **3**(2): p. 182-92.
56. Lachenmaier, S.M., et al., *Intracellular transport of Toxoplasma gondii through the blood-brain barrier*. J Neuroimmunol, 2011. **232**(1-2): p. 119-30.
57. Lang, D., et al., *Chronic Toxoplasma infection is associated with distinct alterations in the synaptic protein composition*. Journal of Neuroinflammation, 2018. **15**(1): p. 216.
58. Wyman, C.P., et al., *Association between Toxoplasma gondii seropositivity and memory function in nondemented older adults*. Neurobiology of Aging, 2017. **53**: p. 76-82.
59. Wang, Z.T., et al., *Reassessment of the Role of Aromatic Amino Acid Hydroxylases and the Effect of Infection by Toxoplasma gondii on Host Dopamine*. Infection and Immunity, 2015. **83**(3): p. 1039-1047.
60. Krishnan, A. and D. Soldati-Favre, *Parasite pathogenesis: Breaching the wall for brain access*. Nat Microbiol, 2016. **1**: p. 16014.

61. Drewry, L.L. and L.D. Sibley, *The hitchhiker's guide to parasite dissemination*. Cell Microbiol, 2019. **21**(11): p. e13070.
62. Dupont, C.D., D.A. Christian, and C.A. Hunter, *Immune response and immunopathology during toxoplasmosis*. Semin Immunopathol, 2012. **34**(6): p. 793-813.
63. Drewry, L.L., et al., *The secreted kinase ROP17 promotes Toxoplasma gondii dissemination by hijacking monocyte tissue migration*. Nat Microbiol, 2019. **4**(11): p. 1951-1963.
64. Pifer, R. and F. Yarovinsky, *Innate responses to Toxoplasma gondii in mice and humans*. Trends Parasitol, 2011. **27**(9): p. 388-93.
65. Carruthers, V.B. and Y. Suzuki, *Effects of Toxoplasma gondii infection on the brain*. Schizophr Bull, 2007. **33**(3): p. 745-51.
66. Ben-Harari, R.R., E. Goodwin, and J. Casoy, *Adverse Event Profile of Pyrimethamine-Based Therapy in Toxoplasmosis: A Systematic Review*. Drugs R D, 2017. **17**(4): p. 523-544.
67. Liu, J., et al., *An ensemble of specifically targeted proteins stabilizes cortical microtubules in the human parasite Toxoplasma gondii*. Mol Biol Cell, 2016. **27**(3): p. 549-71.
68. Hamie, M., et al., *Imiquimod Targets Toxoplasmosis Through Modulating Host Toll-Like Receptor-MyD88 Signaling*. Front Immunol, 2021. **12**: p. 629917.
69. Itani, S., et al., *Imiquimod Reverses Chronic Toxoplasmosis-Associated Behavioral and Neurocognitive Anomalies in a Rat Model*. Biomedicines, 2024. **12**(6): p. 1295.
70. Jeffrey, P. and S. Summerfield, *Assessment of the blood-brain barrier in CNS drug discovery*. Neurobiol Dis, 2010. **37**(1): p. 33-7.
71. Veldhuis Kroeze, E., et al., *In Vivo Models to Study the Pathogenesis of Extra-Respiratory Complications of Influenza A Virus Infection*. Viruses, 2021. **13**(5).
72. Perel, P., et al., *Comparison of treatment effects between animal experiments and clinical trials: systematic review*. Bmj, 2007. **334**(7586): p. 197.
73. Saliba, J., et al., *Development of Microplatforms to Mimic the In Vivo Architecture of CNS and PNS Physiology and Their Diseases*. Genes (Basel), 2018. **9**(6).
74. Brown, T.D., et al., *A microfluidic model of human brain (μ HuB) for assessment of blood brain barrier*. Bioeng Transl Med, 2019. **4**(2): p. e10126.
75. Delsing, L., et al., *Models of the blood-brain barrier using iPSC-derived cells*. Mol Cell Neurosci, 2020. **107**: p. 103533.
76. Sivandzade, F. and L. Cucullo, *In-vitro blood-brain barrier modeling: A review of modern and fast-advancing technologies*. Journal of Cerebral Blood Flow & Metabolism, 2018. **38**(10): p. 1667-1681.
77. Naik, P. and L. Cucullo, *In vitro blood-brain barrier models: current and perspective technologies*. J Pharm Sci, 2012. **101**(4): p. 1337-54.
78. Stone, N.L., T.J. England, and S.E. O'Sullivan, *A Novel Transwell Blood Brain Barrier Model Using Primary Human Cells*. Frontiers in Cellular Neuroscience, 2019. **13**.
79. Baeten, K.M. and K. Akassoglou, *Extracellular matrix and matrix receptors in blood-brain barrier formation and stroke*. Dev Neurobiol, 2011. **71**(11): p. 1018-39.

80. Paradis, A., D. Leblanc, and N. Dumais, *Optimization of an in vitro human blood-brain barrier model: Application to blood monocyte transmigration assays*. *MethodsX*, 2016. **3**: p. 25-34.
81. Furtado, J.M., et al., *Migration of Toxoplasma gondii –Infected Dendritic Cells across Human Retinal Vascular Endothelium*. *Investigative Ophthalmology & Visual Science*, 2012. **53**(11): p. 6856-6862.